CUNY GRADUATE CENTER

QUEENS COLLEGE

Master Thesis

Quantifying psychostimulant-induced Sensitization Effects on Dopamine and Acetylcholine Release across different Timescales

Georg Lange

Graduate Center, City University of New York

January 27, 2023

CUNY GRADUATE CENTER

QUEENS COLLEGE

Master Thesis

Quantifying psychostimulant-induced Sensitization Effects on Dopamine and Acetylcholine Release across different Timescales

by

Georg Lange

Supervisors

Prof. Dr. Jeff Beeler, Dr. Rudolf Faust

Graduate Center, City University of New York

Graduate Center, City University of New York

January 27, 2023

Abstract

Drug-induced behavioral sensitization describes the phenomenon that behavioral response to a drug of abuse is getting stronger if the same psychostimulant is delivered multiple times which is much more pronounced if done in the same environmental context. A proposed neural basis is the formation of an association between contextual cues and the rewarding drug which is mediated by dopamine. Dopamine operates at different timescales and to fully understand dopamine sensitization, it is necessary to investigate dopamine release at slow (tens of minutes) but also faster (sub-second) timescales. But creating a holistic view has been difficult due to a lack of technology that can measure dopamine across various temporal resolutions. We develop an analysis pipeline to expand fiber photometry to measure tonic dopamine activity. We use genetically encoded neurotransmitter indicators to measure extracellular dopamine and acetylcholine activity in the nucleus accumbens of mice. We show that the method is precise enough to measure dopamine sensitization in response to repeated cocaine and amphetamine injections. We then further characterize how dopamine dynamics change in response to psychostimulants. We see that drug-evoked dopamine rises and decays faster in sensitized mice compared to the first injection and that there are more small but less big transients which leads to a smaller fluctuation at a timescale of tens of seconds. We simultaneously record striatal acetylcholine and observe that the frequency and amplitude of transients decrease during sensitization. We also investigate interaction between dopamine, acetylcholine, and movement and report that the relationship between accumbal activity and locomotion gets stronger and that dopamine and acetylcholine interact closely. In addition, we use DeepLabCut and MoSeq to densely annotate behavior. We show that MoSeq can potentially be used to replace locomotor activity with a better measurement of behavioral sensitization.

Acknowledgments

I would like to extend my sincerest gratitude to Prof. Dr. Jeff Beeler, for providing me with the opportunity to research in this lab and for his invaluable contributions, ideas for experiments, and all of the materials I needed for my experiments. I am deeply appreciative of his guidance and support throughout this journey.

I would also like to express my deep appreciation to Dr. Rudolf Faust, for being my scientific mentor and teaching me everything I know about the lab and experimental neurobiology. He not only taught me how to do surgeries, mouse colony management, PCR, and photometry, but also provided me with freedom and support throughout my research. His constant guidance and encouragement were crucial to my success.

I would also like to thank Dr. Youcef Bouchekioua, Federico Gnazzo, Candice Gordon, Kunhee Lee, and my undergraduates Jonathan Nudman and Gaozhen Li for their big help and support. They were always there to assist me with experiments and to engage in meaningful scientific discussions.

Lastly, I would like to thank all of the other members of the Jeff Beeler lab for making my experience such a wonderful one. The supportive environment and camaraderie that exists in this lab is truly special and I am deeply appreciative for having had the opportunity to be a part of it.

Without the support and contributions of all of these individuals, this thesis would not have been possible. Thank you all for your support and help.

Contents

1 Introduction **1**

1.0.1 Psychostimulant-induced Behavioral Sensitization 1
1.0.2 Cholinergic Activity in the Nucleus Accumbens 2
1.0.3 Measurements of Behavioral Sensitization 4

2 Methods **7**

2.1 Animals 7
2.2 Surgery 7
2.3 Fiber photometry 8
2.4 Experimental setups 8
2.5 Data Analysis 9
2.5.1 Detrending of Dopamine Data 9
2.5.2 Removal of Rotary Joint Artifacts 11
2.5.3 Dopamine Rise Time 11
2.5.4 Dopamine Fluctuation 12
2.5.5 Fast Fourier Transform 12
2.5.6 Dopamine Transients 12
2.5.7 Processing of Acetylcholine Data 12
2.5.8 Finding the Onset of Locomotor Activity 12
2.5.9 Statistics 13
2.6 DeepLabCut 13
2.7 MoSeq 14

3 Results **17**

3.1 Locomotor sensitization after repeated injections of cocaine and amphetamine 17
3.2 Photometry recordings reveal dopamine sensitization across different timescales 19
3.3 Dopamine transients during sensitization 21
3.4 Accumbal ACh levels and dynamics change in response to psychostimulants 24
3.5 Interaction between dopamine, ACh, and locomotion 26
3.6 Baseline Acetylcholine predicts Sensitization 28
3.7 MoSeq allows for precise quantification of behavior and describes behavioral sensitization better 31

4 Discussion and Future work **39**

References **41**

5 Supplementary Figures **45**

1 Introduction

Dopamine is thought to convey a reward prediction error [1] that is essential for reinforcement learning. A reward prediction error is the difference between the received and predicted reward. Rewards can be food, water, or shelter, but also abstract things like social reward. When an animal or human receives and unexpected reward or aversion, it is vital to learn from the experience in order to increase rewards which is necessary for survival. Dopamine encodes this information as a reward prediction error. This signal is then used by downstream neurons to adapt. In the nucleus accumbens, an input structure of the basal ganglia deep inside the brain, these downstream neurons are medium spiny neurons (MSN) that can be classified by their dopamine receptor into D1- and D2 MSN. These neurons can change their synaptic weight in response to dopamine - which is thought to be the biological basis of learning. The nucleus accumbens' primary function is to associate stimuli from the environment with rewards - which is necessary to drive behavior to maximize rewards and thus maximize the chance of survival.

Addictive substances drive dopamine release to abnormally high levels. This can be caused by psychoactive drugs that lead to the release of dopamine via different mechanisms or be the result of behavioral stimuli such as addiction to computer games, social media, etc. This abnormally high dopamine level induces synaptic plasticity in MSN of the nucleus accumbens via overexpression of deltaFosB [2]. DeltaFosB is a critical transcription factor that activates pathways for long-term plasticity [3]. The memory of the association between a context or cues and rewarding outcomes is thought to be stored in the cortico-striatal synapse in striatsl MSNs, and this association is abnormally strengthened for addictive substances and is thought to produce the effect of "wanting", or drug-seeking [4].

1.0.1 Psychostimulant-induced Behavioral Sensitization

Drug sensitization describes the phenomenon that with repeated administration of dopamine-acting drugs, the behavioral effect is getting stronger. Strikingly, this effect is much stronger, if a drug is administered in the same context or as a response to the same cues. This means, if a mouse receives an injection of cocaine in context A, the behavioral response during a second injection depends on whether the mouse is exposed again to context A, or to another context B that is different from A [5]. In this work, we repeatedly inject mice with cocaine or amphetamine in an open-field arena, measure locomotor activity using video tracking, and show that locomotor activity sensitizes to cocaine and amphetamine.

How exactly dopamine induces synaptic plasticity has been extensively studied but is still not quite clear. Exposure to cocaine leads to increased D1-MSN and reduced D2 MSN activity and after sensitization, this effect is increased [6]. Especially D1-MSNs are thought to contribute to sensitization. For example, fiber photometry recordings

revealed that D1 activity is increased after the presentation of drug-associated cues, drives drug seeking, prevents extinction and manipulation using DREADs prevents contextual associations to form [7]. Moreover, D1- and D2 MSNs were imaged using a Miniscope. It was observed that there is great variance between individual cells and that likely a subgroup of D1 MSN drives locomotor sensitization [6]. While these recordings were done in the nucleus accumbens, other researchers [8] looked at the dorsomedial striatum and found an activation of both pathways in response to cocaine using fiber photometry recordings with GCaMP. They also observed that presynaptic connections to afferents coming from the orbitalfrontal cortex strengthen during sensitization and that depressing this pathway using a high-frequency stimulation protocol attenuates cocaine-induced locomotor hyperactivity. Although this might be one pathway responsible for increased locomotor hyperactivity after sensitization, it cannot be the primary pathway for cocaine sensitization, because they observed no difference in locomotor activity after a challenge injection without high-frequency stimulation [8]. This is following the established view that cocaine sensitization is context-dependent and that the context-drug association is stored in the nucleus accumbens. Also, dopamine is released in cocaine-conditioned mice after the presentation of cues that predict cocaine and promote drug seeking [9]. In this work, we measure extracellular dopamine release in the nucleus accumbens shell using a genetically-encoded dopamine indicator GRAB-rDA and fiber photometry.

How exactly cue-drug associations are formed is still controversial. DAT-blockers like cocaine and amphetamine block the reuptake of dopamine into the presynaptic cell, so dopamine is cleared slower from the extracellular space and can act longer. This is producing a lasting increase in dopamine levels and it is hypothesized that this long-lasting "tonic" increase evokes synaptic plasticity and can store the context-drug association. Because of D2-autoreceptors, dopamine neurons are inhibited after cocaine which has been shown using fiber photometry recordings in VTA neurons [10]. This supports the hypothesis that drugs of abuse elevate dopamine in a slow and tonic way, while possibly reducing the amount of phasic activity. However, other researchers argue that phasic activity is needed for cue-induced reward-seeking and that only burst firing can achieve the context-drug association to be formed [11].

1.0.2 Cholinergic Activity in the Nucleus Accumbens

Another important neurotransmitter in the nucleus accumbens is acetylcholine (ACh). Acetylcholine is released by cholinergic interneurons, has an important role in associating cues and stimuli with rewards, and is implicated in diseases such as addiction or levodopa-induced dyskinesia [12].

Cholinergic interneurons are local striatal neurons that receive connections from primarily the cortex and thalamus and synapse onto other striatal neurons. They are tonically active and fire in an irregular way at a frequency of around 0-3 Hz (0.7 Hz median)[13]. They are the primary source of acetylcholine (ACh) in the striatum and co-release glutamate [14]. There are several receptors located on striatal cells that are activated by ACh. Dopaminergic VTA neurons express nicotinic receptors on their terminals which can modulate dopaminergic activity [15]. Several different muscarinic receptors are expressed by medium spiny neurons and cholinergic interneurons themselves [16]. Although they only make up 1 % of all neurons in the nucleus accumbens, they densely arborate the structure

and have major modulatory control. For example, they can evoke dopamine release by activating terminals of VTA neurons via nicotinic receptors without the dopamine neuron sending an action potential [17]. The rewarding and addictive effects of nicotine are due to the activation of dopamine neurons via these nicotinic receptors on dopamine terminals [18].

But what is their functional role? Most recordings of cholinergic activity were done in in- or ex-vivo electrophysiological recordings. There, a pause in firing is observed after salient stimuli. For example, in the dorsal striatum, cholinergic interneurons pause in a conditioned motor task [19]. In the ventral striatum, cholinergic interneurons pause after stimuli that are salient or related to reward, either positively or negatively. In other experiments in our lab, we observed long cholinergic pauses in the nucleus accumbens after conditioned cues. The cholinergic pauses can be induced by different neural populations. Gabaergic VTA-neurons for example pause cholinergic interneurons and this enhances associative learning [20]. Other researchers argued that a pause in thalamic and cortical input induces the cholinergic pause and that dopamine only plays a minor role [21]. However, they also argued that dopamine can induce cholinergic pauses if an ACh transient occurs short before the dopamine transient.

An important proposed function of cholinergic interneurons is to open a window for plasticity. As dopamine mediates reward learning but also motivation, it is unclear how MSNs can discriminate between both. One possible idea is that ACh gates dopamine release and striatal plasticity. Recent evidence supports this idea by discovering that cholinergic pauses are necessary to induce striatal plasticity [22].

But besides pauses, also short cholinergic transients have been reported. Those transients are the result of synchronous cholinergic firing. These ACh events occur short before motor movements are initiated in the dorsal striatum, and after salient cues or stimuli that are possibly related to reward in the ventral striatum [23]. ACh transients respond faster to stimuli [21] compared to MSNs and can be caused by thalamic input. It has been proposed that visual stimuli that are predictive of rewards produce ACh transients through a pathway via superior colliculus and thalamus [24]. Thus, one idea about cholinergic function is that ACh events shape dopamine release around salient events such that signal-to-noise ratio is increased and dopamine firing occurs sharp around events related to reward. Recently, it has been proposed that dopamine conveys causal associations about events that cause rewards [25]. Empirical evidence was obtained using dlight recordings in the nucleus accumbens but not VTA dopaminergic cell activity itself. Thus, it might be imaginable that acetylcholine plays a role in shaping this causal signal by invoking information about cues and stimuli, but evidence for this remains to be found. Dopamine also explains behavioral dynamics in response to novel objects and this effect is biggest in the tail of striatum [26]. It is imaginable that this effect is partly driven by the synchronic activity of cholinergic interneurons that are known to respond to salient stimuli, but this is not yet known and thus speculation.

Although there exists evidence that cholinergic pauses are needed to induce plasticity [22], an absence of acetylcholine (which seems to be similar to a huge cholinergic pause) prevents plasticity. For example, silencing cholinergic neurons during cocaine exposure blocks cocaine conditioning [27]. Also, knocking out an acetylcholine transporter in cholinergic interneurons to stop acetylcholine release prevents forming of approach behavior towards conditioned stimuli.

While different functions have been proposed for cholinergic interneurons, there is still a lack of evidence for most. Mainly pauses and short transients were investigated. Proposed functions are that cholinergic interneurons gate plasticity and deliver information and timing of salient cues. Also, it has been proposed that stimuli are associated with outcomes only during cholinergic pauses.

1.0.3 Measurements of Behavioral Sensitization

The key to researching behavioral sensitization is to measure and quantify behavior. Traditionally, locomotor activity has been used to measure the amount of sensitization, because an increased locomotor activity is one of the most pronounced effects of behavioral sensitization to drugs of abuse, but also because it is easy to measure.

Many approaches exist to quantify locomotor activity. Without any technology, distance moved can be quantified if for example an open-field arena is segmented into quadrants and the number of crossings between quadrants is counted. However, human annotation is expensive, error-prone, and can be biased if the researcher is not blinded to the treatment or genotype of the mouse. Thus, other methods have been developed as well. Another simple measurement is to use beam break sensors. These usually work by placing an Infrared (IR) - or laser sender- and receiver in an arm where the mouse can run through. The mouse's body breaks the beam and can be counted easily with simple technology. If the mouse runs more, more beam breaks will be counted. Also, video tracking can be used to determine the location of the mouse in a video and programmatically calculate the real distance traveled. Multiple commercial applications exist such as Ethovision XT, or AnyMaze. EZ-track is an open-source application for the same task [28]. These algorithms usually work by subtracting a static background and applying some simple contrast-enhancing and smoothing techniques and a simple algorithm to find the center of the mouse to extract the mouse's position in a given frame of the video. This software is robust if performed in laboratory settings where the background is static and the mouse is clearly separated by color from the background.

However, it has become more important to look at behavior more holistically. Locomotor activity measured by center-of-mass from a video stream is only a sparse measure of the real motor behavior of the mouse. This can make measurements noisy and increases the number of animals needed for a project. We looked at individual mice during drug sensitization and observe that some animals sensitize behaviorally in form of repetitive behaviors or excessive grooming. Both are clear markers of behavioral sensitization [29], but oppose the measurement of locomotor activity, because the mouse doesn't move when it is grooming.

This calls for better and more fine-grained measurements of behavior and different approaches were developed. DeepLabCut [30] is a method for markerless 3D-pose estimation using artificial neural networks. It makes use of a pose-estimation framework that was originally developed to detect the location of body parts in videos of dancing humans but can also be trained on animal data. DeepLabCut provides a framework to extract and annotate frames of an experimental recording, train a model on these data, and use this model to predict body parts of animals. While many thousands or millions of images are usually needed for Deep Learning, it is often possible to get good results with only a few hundred images, because a pre-trained model is used to accelerate and generalize

training, and because lab settings are usually simple as they usually have a static, monotone background. We used DeepLabCut to get the location of 13 different markers like nose, tail, and limbs, and used this data to calculate locomotion. We specifically used DeepLabCut, because traditional mouse tracking algorithms failed with our experimental setup because of lacking contrast between a black mouse and black background. Pose estimation techniques such as DeepLabCut produce locations of body parts for each video frame and can be used for different tasks. For example, these points can be used directly for data analysis, or be input to other models that for example use these points to cluster the behavior into behavioral syllables [31].

Another approach to finding behavioral syllables is MoSeq [32]. MoSeq is a method to cluster the mouse's behavior into different so-called "syllables" in an unsupervised manner. Syllables denote short 200-400 ms long meaningful behavioral events such as "rear up", "dart", "turn right", or "freeze". MoSeq uses 3D data collected with a Microsoft Kinect camera. The mouse is extracted and aligned and a Principal Components Analysis (PCA) is performed to lower dimensionality. On these features, an Autoregressive Hidden Markov Model (AR-HMM) is trained to cluster the time-series data into syllables that are equivalent to specific motor movements of the mouse. HMMs are generative sequence models that were developed for Natual Language Processing and other time-series data and assume that observations are a consequence of a hidden, unobservable process whose outcome is probabilistic and only depends on the previous state.

2 Methods

2.1 Animals

16 wild-type animals were used for psychostimulant-induced locomotor sensitization experiments (8 male, 8 female, C57BL/6 Jackson Laboratory, 20-25 weeks old). All mice were age and sex-matched with their respective control group. Animals were individually housed under a 12 h day/night cycle, All experiments were approved by the Queens College Institutional Animal Care and Use Committee.

2.2 Surgery

Surgical instruments were autoclaved on a 20 min cycle before each surgery. The surface of the operating table, the stereotaxis, the microscope, and all other appliances and items used for surgery were thoroughly wiped down with clidox and 70 % ethanol. The surgeon used aseptic surgical techniques and sterile gloves, a face mask, and a sterile pad. Instruments were kept sterile in hot beads throughout the procedure.

Animals were anesthetized with ketamine/xylazine (90-120 mg/kg and 5-10 mg/kg, respectively, I.P.) and after 5 minutes placed into an isoflurane chamber (4 % for induction) for 3 more minutes. For maintenance, a level of 1-1.2 % isofluorane was kept. Before the procedure and during surgery, the animal was continuously monitored for body temperature and breathing. The preparation of the animals for surgery was only started after the animal completely lost its righting and toe pinch reflex. The hair was shaved over the incision areas and the scalp was cleaned and sterilized using sterile water and chlorhexidine and repeated twice. In addition, bupivacaine (1.25-2 mg/kg) was injected subcutaneously. Then, the mouse was placed into the stereotaxis. To continuously maintain the anesthesia, Isofluorane in oxygen was delivered via a nose cone and kept at a rate of 1-1.2 %. Paralube was applied to the eyes to prevent them from drying out. Then, the scalp was washed three times with 70 % alcohol and Betadine.

A single continuous incision was made along the rostral-caudal axis and the skin was separated and fixed with clamps. The exposed skull was dried and leveled such that Bregma and Lambda had a vertical difference of less than 0.1 mm. Then, the target was stereotactically identified and a small craniotomy was drilled using a dental drill without damaging the dura or the cortex. Then, the dura was opened using a small tool. A Nanofill syringe was loaded with virus and positioned stereotactically. The virus was stored aliquoted upon arrival and stored at -80 degrees. After thawing, it was kept on ice and used within 3 days. The syringe was lowered to the target position at a speed of 0.5-1 mm per minute. Then, AAV was pressure injected at a rate of 46 nl / min. After the injection was complete, we waited for 10-15 minutes for the virus to dissociate and then gradually removed the syringe at a speed of 0.5-1 mm/min. The implant was sterilized

and positioned stereotactically. It was then slowly lowered to the target position inside the brain at a speed of 0.5 - 1 mm per minute. Metabond (dental cement) was applied to form a cap around the implant, thus fixing the implant at the skull. Then, the skin was sutured and Betadine was applied. Additionally, buprenorphine (0.1 mg/kg SC) and carprofen (5 mg/kg IP) were administered. The mouse's body temperature was monitored during the hours past surgery and it was placed under a heat lamp. After surgery, the animal was monitored until fully awake. The mouse was singly housed after surgery and during experimental procedures. The mouse was monitored every 12 hours for signs of complications, illness, or distress.

To measure dopamine and acetylcholine, we injected GRAB-rDA [33] and GRAB-ACh3.0 [34] with a titer of $2x10^13GC/ml$ and a volume of 175 nl per virus (350 nl per surgery) unilaterally (left hemisphere) into the nucleus accumbens shell at (AP 1.3 mm, ML -0.7 mm, DV 4.4 mm).

We fabricated fiber optic implants in-house using 200 um fibers with a numerical apperture of 0.37 (Thorlabs, FT200UMT - 0.39 NA, Ø200 µm Core Multimode Optical Fiber) and ceramic ferrules with dimensions of 1.25 mm x 6.4 mm and a bore size of 230 um (Thorlabs, CFLC230-10). The fiber was cut to the desired length and glued into the ferrule. Then, both ends of the fibers were polished until they had an efficiency of > 85 %.

2.3 Fiber photometry

All photometry recordings were performed with a commercial photometry system by Neurophotometrics (FP3002). Three LEDs at frequencies of 560 nm (red-shifted indicators for dopamine), 470 nm (green indicators for acetylcholine), and 410 nm (isosbestic control signal) were used. Only one LED was on at a time and recordings were performed at a frequency of 90 Hz, which effectively yields 30 Hz. LED light was guided into a low-autofluorescence patch cord fabricated by doric lenses. For open-field testing, we used a pigtailed rotary joint from doric lenses (FRJ_1x1_PT___0.15m_)to prevent the patch cable from entangling during heavy locomotor activity. Light emitted by the indicator was guided back to the photometry system via the same fiber-optic patch cable. There, the light was separated by wave length using dichromic mirrors.

To allow for sensor expression, recordings were done at least 4 weeks after virus injection. Light intensity at the tip of the fiber was selected such that the signal covers a high amount of the dynamic range of the camera while being as low as possible to reduce the photobleaching of the sensor. For recordings with a rotary joint, we used 50 uW.

2.4 Experimental setups

All experiments were performed in the dark. Except for the IP injection, no researcher was present in the room for the entire session. Video, Depth- and neural data were recorded simultaneously. For video recordings, we used an ordinary IR camera (ELP Camera USB 1080P), to collect an HD video in the dark. For depth recordings, a Microsoft Kinect 2 was used. Photometry data were recorded as mentioned above. A 3D-printed mount was used to fix the rotary joint and keep the patch cable at optimal length for

long recordings. To synchronize video and photometry data, both data streams were simultaneously collected using Bonsai, a graphical programming software specialized in acquiring data from psychological experiments. To synchronize depth data to photometry, both acquisition programs stored DateTime values for every data point collected.

N = 16 wild-type mice were tested for drug-induced locomotor sensitization via the following procedure. Animals were habituated to an open-field arena (black spray-painted, 21 cm in diameter), to the fiber-optic patch cable, and to IP injections on three subsequent days. To reduce stress during the IP injection, mice were habituated to the researcher's hand daily starting 2 weeks before the experiments. All sessions, including the habituation sessions, were 60 minutes long with the IP injection after 10 minutes. IP injections were consistently kept below one minute, and data collected in that time window were tagged and later removed from the analysis.

After habituation, we recorded a 60-minute baseline with a saline injection after 10 minutes for every mouse. After three days, we recorded an injection of cocaine (20 mg/kg, n = 5), d-amphetamine (2 mg/kg, n = 5), or saline (n=6) via the same protocol. We chose to leave at least 3 days between recordings as we measured in a small prior experiment that this was the time needed for the sensor (GRAB-rDA) to fully recover from photobleaching. We repeated this for five subsequent days. We didn't record injections 2, 3, and 4 (for the sensor to recover), but recorded injection 5. Then, after 7 days without any injection, we recorded a challenge injection using the same dosage. Mice of the saline group were injected with cocaine (n = 3) or d-amphetamine (n = 3) during the challenge. One recording of one mouse was removed from analysis due to complications after the IP injection.

2.5 Data Analysis

All data analyses were custom-made and written in Python using Pandas, Numpy, Scipy, and Pingouin unless stated otherwise.

2.5.1 Detrending of Dopamine Data

Fluorescence varies within and between sessions due to different effects of photobleaching or other artifacts. Thus, the key to a correct analysis of dopamine across longer timescales is the correct removal of these effects. In the subsequent paragraphs, we describe how we performed detrending and how we verified the correctness.

First, we measured the size of different artifacts. We recorded a patch cable that was not connected to an implant and pointed it into the dark. The photometry didn't pick up any fluorescence. All pixels of the camera were 0 which suggests that the autofluorescence of the patch cable used was below the detection threshold of the camera. We further did the same test in an awake-behaving mouse who was implanted but had no sensor expression to determine the amount of autofluorescence emitted by brain tissue and implant. Again, we found that the fluorescence emitted was below the detection threshold. Thus, we reasoned that the remaining fluorescence must come from the sensor itself and that a slow exponential decay is only caused by the photobleaching of the sensor.

To test this, we injected a dopamine-insensitive version of the sensor, GRAB-rDA-mut, in 4 mice. This sensor is equivalent to GRAB-rDA except for a single point mutation in the dopamine binding site that renders it insensitive to dopamine. The baseline fluorescence is similar to the baseline fluorescence of GRAB-rDA and we observed the same exponential decay and reasoned that this decay is caused by the photobleaching of the sensor.

We aimed at removing this exponential decay to extract the neural data. To do so, our goal was to collect data with no other artifacts that influence baseline fluorescence. One problem identified is bending loss. Bending loss is a result of the physics of the optic fiber. An optic fiber consists of a core and a cladding that have different refractive indices. The light inside the fiber is then reflected at the intersection between the core and cladding and does not exit the fiber. However, when the fiber is physically bent, light can exit the fiber at the bending location because there, the angle of attack is greater than the maximum angle for complete reflection. Bending loss is especially a problem with LED light and light emitted by the sensor because it overfills the fiber. While in industry, lasers are preferred for that reason, this is not possible here. Bending loss can happen when the mouse is moving a lot and the patch cable gets entangled. Because of the highly increased locomotor activity during psychostimulant exposure, this was a significant problem. To solve this and prevent the bending loss, we installed a rotary joint that made it possible for the patch cable to rotate together with the mouse. Using mice with GRAB-rDA-mut, we confirmed that no bending loss occurred and that there were no other significant sources of artifacts that influence baseline fluorescence.

Photobleaching is caused by covalent changes in the fluorophore caused by long or high exposure to light that makes the molecule non-fluorescent. That means, fluorescent changes caused by the neurotransmitter of interest also decrease. To compare signals between sessions, it is important that changes in signal mean a similar change in transmitter concentration. In a prior experiment, we experimented with the length between recordings. We noticed that GRAB-rDA recovers from photobleaching completely after 3 days. Thus, we left at least 3 days in between subsequent recordings to allow for recovery of fluorescence. After the experiment, we investigated the raw fluorescent data and verified that for all sessions, fluorescence and degree of photobleaching are similar.

To estimate a baseline fluorescence, we fit a bi-exponential decay to the data for all baseline sessions where saline was injected. For the other sessions, we can't do this because the significant and prolonged increase in dopamine after injection of psychostimulants impacts the regression negatively. There, we excluded the first 40 minutes after injection from regression as this was the time window where dopamine was increased. Because the exponential decay of photobleaching was similar across sessions per mouse, we used the regression of the baseline recording and made a linear fit to the data (40 minutes after injection excluded) of the other three recorded sessions. We validated this approach with sessions recorded from mice with GRAB-rDA-mut and with sessions from the saline group, where dopamine levels were stable throughout the session. We then subtracted the regressed baseline from the raw data to remove the photobleaching-induced decay of fluorescence.

To better compare signals, we calculated z-scores (zdFF) by subtracting the median and dividing by the standard deviation. Because short big dopamine transients can negatively alter the calculation of z-scores, we excluded 5 % of the highest and 5% of the lowest values. Also, we only used the 10-minute baseline to determine the median and standard

deviation as the big drug-induced dopamine increase would make comparisons between animals and sessions impossible.

2.5.2 Removal of Rotary Joint Artifacts

The rotary joint can introduce periodic increases and decay in fluorescence when it turns, as even tiny imperfections cause big changes in fluorescence. To keep artifacts as small as possible, we used a rotary joint that was pigtailed by the manufacturer and tested for low rotational variance. While this significantly decreased the amplitude of artifacts, it was still necessary to remove the remaining artifacts.

We used the isosbestic signal to remove the artifacts. The isosbestic is the signal collected when the sensor is excited at a wavelength of 410 nm. Most genetically encoded indicators emit a similar amount of fluorescence independent of whether the transmitter is present. Thus, data collected from the isosbestic includes rotary joint artifacts, but not neural data.

Artifacts in the isosbestic signal are different in absolute brightness and scale. Thus, it is necessary to shift and scale the data such that artifacts in the isosbestic and signal are of same amplitude. To find a good fit, we temporarily removed slower changes in fluorescence such that isosbestic and signal are both flat and a good scale can be found. The artifacts were removed in the following way. First, we removed slower changes in fluorescence caused by drug-induced dopamine release using adaptive iteratively reweighted penalized least squares (airPLS) [35]. This method estimates a baseline by iteratively changing weights of sum square errors between the fit and the raw data in an adaptive way. We set lambda to 1e4 and used an available python implementation of the algorithm [35]. We then used a non-negative robust linear regression to align the isosbestic to the signal. Because artifacts were different in amplitude between the isosbestic and the signal, we smoothed the data with a 450 ms moving average and made a linear fit, and scaled the isosbestic to match the signal. Then, we subtracted the smoothed and scaled isosbestic from the detrended unsmoothed dopamine signal. Important to note is that we removed slow changes in fluorescence earlier to find how much the isosbestic needs to be scaled but now subtract the scaled and fitted isosbestic from the initial dopamine signal. Thus, we get the dopamine signal with all slow changes conserved, but exclude artifacts. To evaluate this approach, we recorded mice with GRAB-rDA-mut for two sessions, one of them with an injection of cocaine or amphetamine. We observed that rotary joint artifacts increase on psychostimulants due to increased locomotion and that our algorithm is able to almost completely remove these artifacts.

2.5.3 Dopamine Rise Time

We measured how fast dopamine rises within the first few minutes after injection. To quantify this, we calculated the time when dopamine was rising the fastest on average. Dopamine traces were smoothed with a 60-second moving average to filter out the phasic activity. The timescale of phasic activity is subsecond (rise of dopamine transients) to multiple seconds (fall of dopamine transients, bout of transients). Tonic activity is typically observed using microdialysis and changes over multiple minutes. Thus, the 60-second moving average smoothed out the phasic activity while keeping slower changes. Then,

the derivative was calculated and the maximum was selected as the time of the fastest dopamine climb.

2.5.4 Dopamine Fluctuation

To get the dopamine fluctuation across a timescale of tens of seconds, the dopamine data were first smoothed with a 10-second moving average. Then, the standard deviation was calculated using another moving window. Data from 5 minutes until 30 minutes after injection were included.

2.5.5 Fast Fourier Transform

The data were smoothed with a 160 ms moving average. Then, the fast Fourier transform was calculated during the 10-minute baseline and for 10 minutes after injection separately. The NumPy function np.fft() was used for the Fourier transform.

2.5.6 Dopamine Transients

We selected dopamine transients as fast monotonic increasing rises that are at least one z-score in amplitude. The threshold of one z-score was selected to minimize contamination by fluorescent noise while not excluding real transients. Dopamine data were smoothed with a 160 ms moving average.

2.5.7 Processing of Acetylcholine Data

Our acetylcholine measurements are characterized as short and sharp spikes that occur at a frequency of 1-2 Hz but are unpredictable (they exhibit no obvious regular pattern). Because we only looked at phasic activity throughout this study, we didn't apply the mentioned processing pipeline that we developed to analyze dopamine data across timescales to acetylcholine. Rather, we used the airPLS [35] to remove photobleaching and artifacts. We used a low lambda of 9 that produced a rapidly changing baseline to remove artifacts from photobleaching as well. This was possible because acetylcholine spikes occur at a much faster timescale than artifacts from the rotary joint. We then calculated z-scores by subtracting the median and dividing by the standard deviation. Then, local peaks were identified as ACh transients. We filtered the events such that only events with an amplitude of 1.5 and a distance of the neighboring event of at least 130 ms.

2.5.8 Finding the Onset of Locomotor Activity

Because we sought to only identify locomotor activity and not any movement, we used the basis of the tail as a proxy for locomotor activity. We smoothed the movement data with a 160 ms moving average and calculated the derivative. Then, local peaks were extracted and used as locomotor activity onset if they were at least 0.5 in height and 300 ms apart from other movement onsets.

2.5.9 Statistics

Independent and paired t-tests were performed with Scipy using the function stats.ttest_ind() or stats.ttest_rel(). ANOVAs were performed with the Pingouin package using the function pg.mixed_anova(). A type 2 ANOVA was used for unbalanced datasets. To compare groups with different variances, we used Welch's t-test.

2.6 DeepLabCut

The genetically encoded transmitter indicators that we used for this project are excited by and emit light into the visual spectrum. Thus, it is possible that other light sources, for example, room light, introduce noise and artifacts in the recording. To prevent this, we performed all experiments in the dark. Also, this is more natural for mice as they are more active at night. To get a video recording, we used an ordinary commercially available IR camera (ELP Camera USB 1080P) that collects a full-HD video of the mouse behaving in the bucket.

Although the mouse is clearly visible in the video, we found that established mouse tracking libraries (we tried EZ-track) fail to detect the position of the mouse properly even after thoroughly finetuning all parameters. This is because the algorithms used rely on a difference in hue between the mouse and background as opposed to e.g. contrast between the mouse's shape and the background. To deal with these problems, we decided to use DeepLabCut instead.

DeepLabCut [30] is a method for markerless pose estimation using deep learning. It is implemented as a software library that contains functionality to process videos, label frames, train an image model for pose estimation, and generate output movies. For all analyses, DeepLabCut version 2.3.0 was used together with NVIDIA CUDA 11.7, cuDNN 8.5.0, and TensorFlow 2.7.1. Training and inference were done on an accelerated computing instance on Amazon Web Services (AWS) with an A10G GPU (ml.g5.2xlarge). We uniformly extracted 10-20 frames per video and added 40 images that showed edge cases. We then manually annotated in total 279 frames with 13 markers for different parts of the mouse's body. We labeled the tip of the nose, both eyes, both ears, four points on the tail, and all limbs. For the nose and base of the tail, we labeled every image and estimated the position if the body part was occluded. For all other markers, we only labeled body parts that were visible. Successively, the model learned to assign a marker for the nose and base of the tail for every image with a high probability, but for other body parts only if it is visible in the image.

We used a ResNet-50 [36] that was pre-trained on ImageNet data and finetuned it using our labeled data. We found that the model performed poorly and had difficulties learning when trained on the full HD image, so we resized the images to a fifth of the original size. We trained for 230000 iterations with a decaying learning rate. Else, we used default parameters provided [30]. The final training error (root mean squared error) is 2.79 pixels, the test error is 2.98 pixels. For points with a probability cutoff of 0.6, the training error was 2.04 pixels, and the test error 2.81. This is a near-perfect result as the human annotations are probably less precise than 2 pixels.

After finetuning, we did inference for all 63 videos to get positions for every body part in every frame. We applied a posthoc filter to smooth the data. To calculate the distance moved, we calculated the euclidean distance between subsequent frames.

2.7 MoSeq

The Kinect camera was mounted 69 cm above the ground of the open-field arena. The bucket was thoroughly sanded and spray-painted in black with Krylon Acryli-Quik ultra flat spray paint (K01602A07) to prevent IR glares. Without it, the light would get reflected at the surface of the bucket and confound the data. Data were collected with a C#-based user interface provided by the Robert Datta Lab[32]. The background was masked with an elliptic filter and the mean depth was subtracted from all images to remove the background and only keep pixels that are part of the mouse. Then, a pre-trained model provided by the MoSeq team was used to crop the image and to align the mouse such that the nose was always on the right side of the image. To deal with the fiber optic cable, we used the model "flip_classifier_k2_largemicewithfiber.pkl" provided by the MoSeq team[32] to align the mouse correctly. For further analysis, we used default parameters unless specified here. To further deal with remaining artifacts from the fiber optic cable, we used a tracking model to decrease the likelihood that the cable is falsely identified as the mouse, and we used a 5x5 cable filter. We then screened the output videos for anomalies using MoSeq functionality. We verified that the mean and standard deviation of floor area, length, height, and speed was reasonable for all sessions (Suppl. Figure 5.4). We excluded one session that we identified as an outlier. After, videos were reduced to 10 dimensions via PCA. To deal with occluded portions of the image because of the cable, we performed iterative missing data PCA as described[37]. The principal components were visualized (Suppl. Figure 5.6) to validate the correctness. We also calculated fingerprints for all sessions that included position, speed, height, and length (Suppl. Figure 5.5) and it was visually confirmed that all measures were in a reasonable range. All principal components seemed to be related to the mouse's body and not to e.g. the cable (Suppl. Figure 5.6). Further, we found that the first 5 principal components explain 91.5 % of the variance, which is more than sufficient for further modeling.

We then applied the PCA to all included sessions and fit the AR-HMM on them as described elsewhere [32]. We first ran a scan to find the optimal kappa value. The kappa value influences syllable length and is thus important to get meaningful behaviors. We trained 15 models with different kappa values for 100 iterations and selected a kappa value of 500000 as it yielded the most reasonable syllable length and was close to the PCA changepoints. Then, we trained a model for 500 iterations. We trained a model with and without a robust version of the AR-HMM with a student's t-distribution and selected the robust model as the final model, based on the observed quality of the syllables. We performed extraction, training, and PCA on a DGX-1-like system with 192 CPU cores.

The model clustered the data into 72 different syllables, out of which 61 were used because they explained more than 99 % of the syllable usage. After training, we performed inference on all sessions to annotate all frames with syllables. To evaluate the meaning of each syllable, we first computed crowd movies. There, 12 occurrences of the same syllable were randomly selected and a 3-second long video of the mouse around that syllable was

extracted. Then, the 12 videos were overlayed to visualize all syllables at the same time. A red marker was used to indicate the time the syllable was detected as each syllable has a different length for each occurrence. These crowd movies were used to assign a syllable name to each. The final syllable names are shown in Figure 3.8C.

3 Results

3.1 Locomotor sensitization after repeated injections of cocaine and amphetamine

Before studying dopamine and ACh characteristics and interaction during drug sensitization, we developed a sensitization schedule and tested behavioral sensitization in an open-field arena. We repeatedly exposed mice to cocaine (20mg/kg, I.P.), amphetamine (2mg/kg, I.P.), or saline. For every mouse, we recorded neural and behavioral data (Figure 3.1**A, B**) for a 60-minute baseline (saline), first and fifth psychostimulant injection, and a challenge after 7 days without injections. For every injection, we recorded 10 minutes before injecting. During the challenge, animals of the saline group received psychostimulants as well (Figure 3.1**A**).

We simultaneously recorded behavioral and neural measurements. We captured video data, and 3D point clouds using a Microsoft Kinect for later fine-grained behavioral analysis with MOSEQ and fiber photometry data (Figure 3.1**B**). We trained an artificial neural network using DeepLabCut [30] to detect specific points of the animal's body. We manually annotated 279 images with locations of the nose, eyes, ears, fore- and back limbs (if visible) as well as four parts on the tail. We then used the DeepLabCut framework to finetune a pre-trained ResNet-50 on our annotated data. (Figure 3.1**C**) We then used the model to predict the location of all body parts for all frames of our recorded videos. We found that the model performed well with a test error of less than 3 pixels and that no big jumps of body markers occurred which could hint to artifacts. Mice exposed to cocaine and amphetamine were primarily running in circles while other animals were exploring the arena in a slower and less circular way (Figure 3.1**D**).

We used the marker at the base of the tail to quantify locomotion. Locomotion is directional movement that enables the mouse to move from one location to another. While the head can move when the animal is not locomoting, for example by doing head turns, rears, sniffing behaviors, or grooming, the base of the tail largely translates to movements across space which makes it a good measurement for locomotion. During the baseline session, none of the animals increased locomotion after the injection. There was a slight downward trend as the mice spend more time in the bucket, some of the mice even fell asleep towards the end of a session (Fig 3.1**F**, suppl. Figure 5.1). After injection of cocaine or amphetamine, locomotor activity rapidly increased and slowly decayed towards baseline levels as the session went on (Figure 3.1**F**). We saw a clear sensitization on the individual level (Figure 3.1**E**, suppl. Figure 5.1) and on average (Figure 3.1**G**). A mixed ANOVA with baseline, injection 1, injection 5, and challenge as repeated measures and treatment as the between-subject condition yielded significant main effects for treatment ($F = 19.58$, $p = 0.000166$) and session ($F = 42.74$, $p = 5.9e\text{-}12$) and an interaction between treatment and session ($F = 6.89$, $p = 0.0000626$). Post hoc pairwise independent t-tests

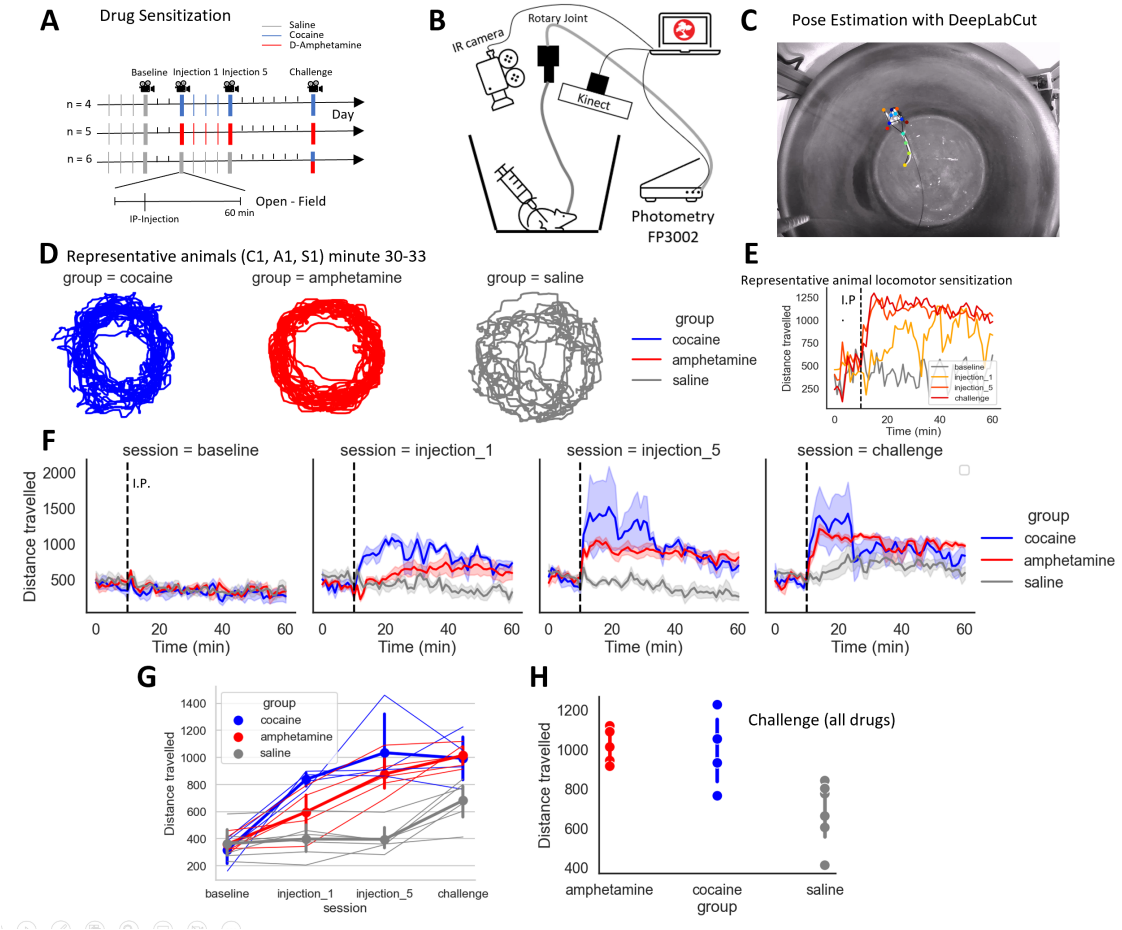

Figure 3.1: Locomotor sensitization after repeated injections of cocaine and amphetamine
A Overview of experimental procedure for psychostimulant-induced locomotor sensitization **B** Overview of recording setup **C** Representative image that shows body markers annotated by a model trained with DeepLabCut **D** Three representative traces of locomotor activity, measured at the base of the tail. Graphs show the position of the mouse in the open-field arena for 3 consecutive minutes **E** Locomotor activity of a representative animal of the cocaine group, measured at the base of the tail. Locomotor activity was grouped into 1-minute bins and averaged. The color indicates the four recording sessions of the same mouse **F** Locomotor activity averaged per group and session **G** Mean distance traveled in the first 20 minutes after I.P. injection. Thick lines denote the group average, fine lines represent individual animals **H** Mean distance traveled in the first 20 minutes after injection during the challenge recording. Animals of the saline group received cocaine or amphetamine during the challenge injection. All error bars denote the .95 confidence interval for the mean, calculated by bootstrapping with 1000 iterations.

revealed significant differences between cocaine and saline (injection 1: p = 0.000194, injection 5: p = 0.0161), amphetamine and saline (injection 1: p = 0.07, injection 5: p = 0.00045), and between cocaine and amphetamine only during the first injection (injection 1: p = 0.033, injection 5: p = 0.368). The effect of amphetamine on locomotion on the first day was smaller compared to cocaine. (Figure 3.1**F, G**).

To test for locomotor sensitization, we compared locomotor activity during the challenge between groups (Figure 3.1**H**). For the challenge, saline animals received either cocaine (n=3) or amphetamine (n=3). We found that locomotor activity was significantly increased for sensitized animals. Pairwise t-tests revealed a significant increase between cocaine and saline (p = 0.04), amphetamine and saline (p = 0.0024) but not cocaine and amphetamine (p = 0.85). We also investigated whether locomotor activity increases between injection 1 and challenge for the cocaine and amphetamine group. A paired one-sided t-test showed a significant increase for the amphetamine group (p = 0.0037) but not for cocaine (p = 0.109). We found that this was the case because some of the animals exposed to cocaine increased their grooming behavior.

3.2 Photometry recordings reveal dopamine sensitization across different timescales

To detect dopamine and ACh dynamics, we injected 16 mice with adeno-associated virus (AAV) in the nucleus accumbens shell (NAcSh) and expressed the dopamine sensor GRAB-rDA and the ACh sensor GRAB-Ach3.0 (Figure 3.2**A**). We then implanted an optical fiber and measured fluorescence changes with fiber photometry. We detrended dopamine data as described in 2.5.1.

First, we sought to reproduce findings from microdialysis studies and determine the degree of dopamine sensitization. There, multiple researchers reported that dopamine concentration is increased in sensitized mice [38]. We were able to see sensitization effects in the dopamine data for individual mice for both amphetamine and cocaine (Figure 3.2**B, C**). To quantify dopamine levels, we calculated the area under the curve for the first 20 minutes after injection. All four cocaine mice and 3 of 5 amphetamine mice showed increased dopamine levels for injection 5 and challenge compared to the first injection (Figure 3.2**D**). To test for dopamine sensitization, we compared dopamine release during the challenge injection between the sensitized mice and the saline group, which received cocaine or amphetamine for the first time during the challenge. We reported a significant increase for both the cocaine group (p = 0.00231, independent one-sided t-test) and the amphetamine group (p = 0.0347, independent one-sided t-test). After this reproduction from previous studies, we investigated changes that might happen at faster timescales. Microdialysis is poor in temporal resolution, with 1 data point every 1-5 minutes. On the other end of the spectrum, fast-scan cycling voltammetry (FSCV) or photometry is often used to detect transient changes on a subsecond scale but fails at detecting slower changes because of a changing baseline (FSCV) or photobleaching (photometry), respectively. Here, we proved that it is possible to use photometry to detect changes that are tens of minutes long.

We visually compared how big transient vs drug-induced tonic changes are (Figure 3.2**B, C**: the thick lines are a 30-second moving average whereas the transparent lines

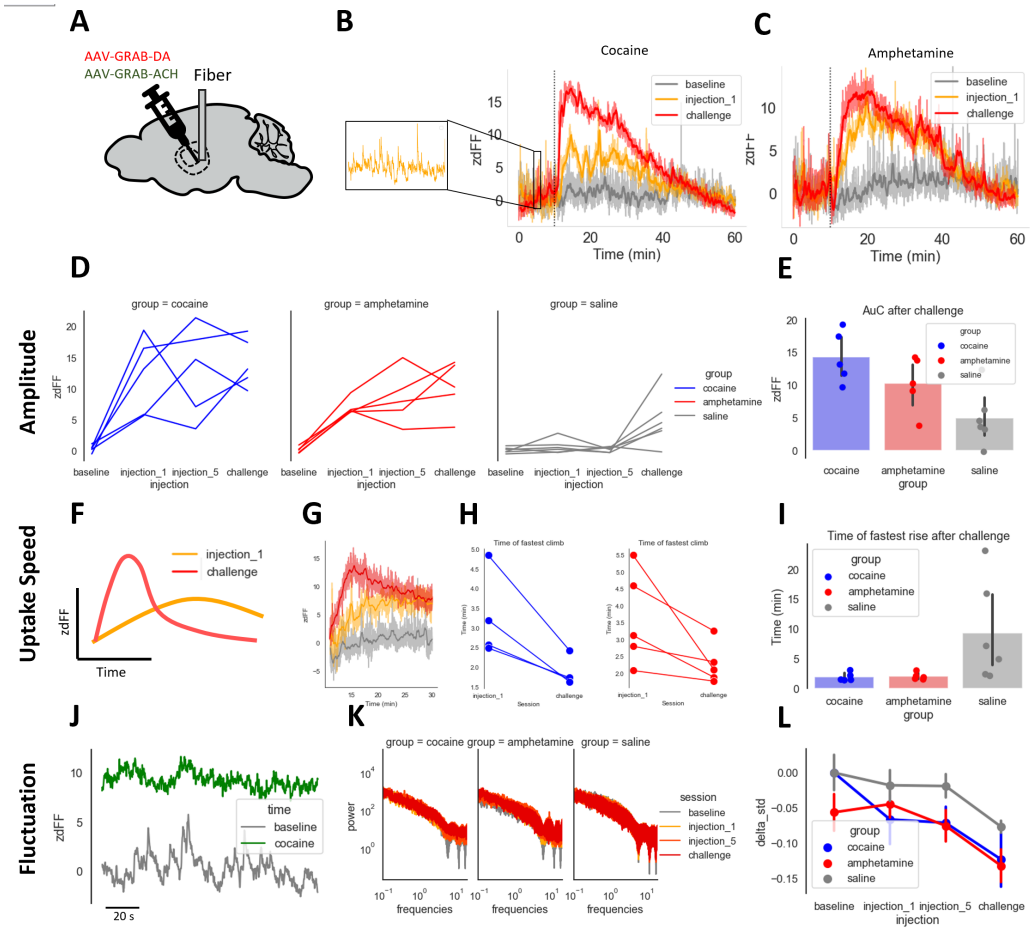

Figure 3.2: Photometry recordings reveal dopamine sensitization across different timescales

A Genetically-encoded transmitter indicators for dopamine (GRAB-rDA) and acetylcholine (GRAB-ACh) were injected into the nucleus accumbens shell, and an optic fiber (200 um) was implanted above the injection site to measure fluorescent changes of the indicators. **B** Left panel: Representative trace of recorded standardized fluorescent changes of dopamine during 60 seconds. Right panel: Dopamine activity of a representative animal over the full 60-minute recording for baseline, injection 1, and challenge. Thick lines mark the 60-second moving average, transparent lines the unsmoothed data **C** Same as B, but for an animal of the amphetamine group **D** Average dopamine activity for every experimental group across sessions. The mean is calculated from 0-20 min after injection. **E** Average dopamine activity during the challenge injection. Saline animals received either cocaine or amphetamine during the challenge. Dopamine is significantly increased for cocaine ($p = 0.00231$, independent one-sided t-test) and amphetamine ($p = 0.0347$, independent one-sided t-test) compared to the saline group. **F** Hypothesis. We investigate whether not only dopamine amplitude changes during sensitization, but also uptake speed **G** Representative animals that show faster dopamine increase for challenge **H** Time of biggest slope per animal; cocaine animals in blue ($p = 0.0353$, paired t-test), amphetamine in red ($p = 0.0705$, paired t-test) **I** During the challenge, dopamine increase is significantly faster in sensitized mice (cocaine: $p = 0.0433$, amphetamine: $p = 0.0451$, independent t-test, corrected for unequal variance using Welch's test) **J** Dopamine trace of a representative animal before and after injection of cocaine **K** Fast Fourier Transform of dopamine traces from 0 – 50 min after injection averaged across animals and sessions **L** Difference in dopamine fluctuation compared to the 10-minute baseline before injection. Dopamine fluctuation is calculated as the standard deviation across a 30-second moving average window on a smoothened dopamine signal. Error bars show s.e.m. A mixed ANOVA revealed a significant main effect for the session ($F = 9.556$, $p = 0.000074$)

are the unsmoothed data including phasic activity). Remarkably, dopamine rises to a level consistently above that of the highest transients during the 10-minute baseline before injection. This is interesting because most studies that analyze transient data baseline individual traces to a short baseline of a few seconds before trial, ignoring the overall dopamine activity completely. Of course, cocaine and amphetamine raise dopamine to abnormally high levels, but this data shows that also investigating tonic dopamine activity when analyzing short trials should at least be considered.

Next, we were wondering whether sensitization produces changes on faster timescales as well. First, we observed that sensitized mice increase their locomotion faster (Figure 3.1**F**) and we investigated whether this is true for dopamine as well. We hypothesized that in addition to the increased amplitude, the dopamine rise after injection is faster and that the decay happens earlier as well. This effect was clearly visible for individual mice (Figure 3.2**G**) and we quantified the time of the steepest slope by finding the argmax of the gradient. As a result, we confirmed that the time of the fastest dopamine rise shifted forward for all animals (Figure 3.2**H**) (cocaine: $p = 0.0353$, amphetamine: $p = 0.0705$, paired t-test). We also compared sensitized mice to the saline group during the challenge and observed a significant difference for both groups (Figure 3.2**I**) (cocaine: $p = 0.0433$, amphetamine: $p = 0.0451$, independent t-test, corrected for unequal variance using Welch's test).

Second, we investigated whether fluctuation in dopamine changes. Dopamine levels are changing on a subsecond scale and we hypothesized that the amount of variation could be lower because DAT is blocked by cocaine or amphetamine, preventing the dopamine signal from being sharp (Figure 3.2**J**). We calculated a fast Fourier transform of the data to investigate how different wavelengths change in power (Figure 3.2**K**). Interestingly, we discovered that fast frequencies seem to increase in power and we reasoned that small, fast transients increase after psychostimulant injection. To investigate how dopamine fluctuates on slower timescales, we smoothed the data with a 10-second moving average window and took the standard deviation of the smoothed signal. We then plotted the change in standard deviation between the 10-minute baseline and a time window of $5 - 30$ min after injection (Figure 3.2**L**). We found that change in standard deviation decreased as mice sensitized (significant main effect for the session: $F = 9.556$, $p = 0.000074$, mixed ANOVA), suggesting that large dopamine fluctuation over tens of seconds decreases after cocaine and amphetamine, but not small, fast transients.

3.3 Dopamine transients during sensitization

Although dips and ramps have been observed, most dopamine activity can be described by transients that are characterized by a fast rise and a slow, exponential decay. After discovering changes in dopamine fluctuation, we were interested in whether they can be attributed to a change in transients, and if transients change during sensitization. Thus, we sought to algorithmically extract the time and size of dopamine transients.

Several approaches have been used in the existing literature. First, researchers defined transients as local peaks exceeding a manually set threshold. [39]. We investigated this method but concluded that it's not suited to extract dopamine transients. This is because transients occur at different timescales and different amplitudes. This makes it difficult to

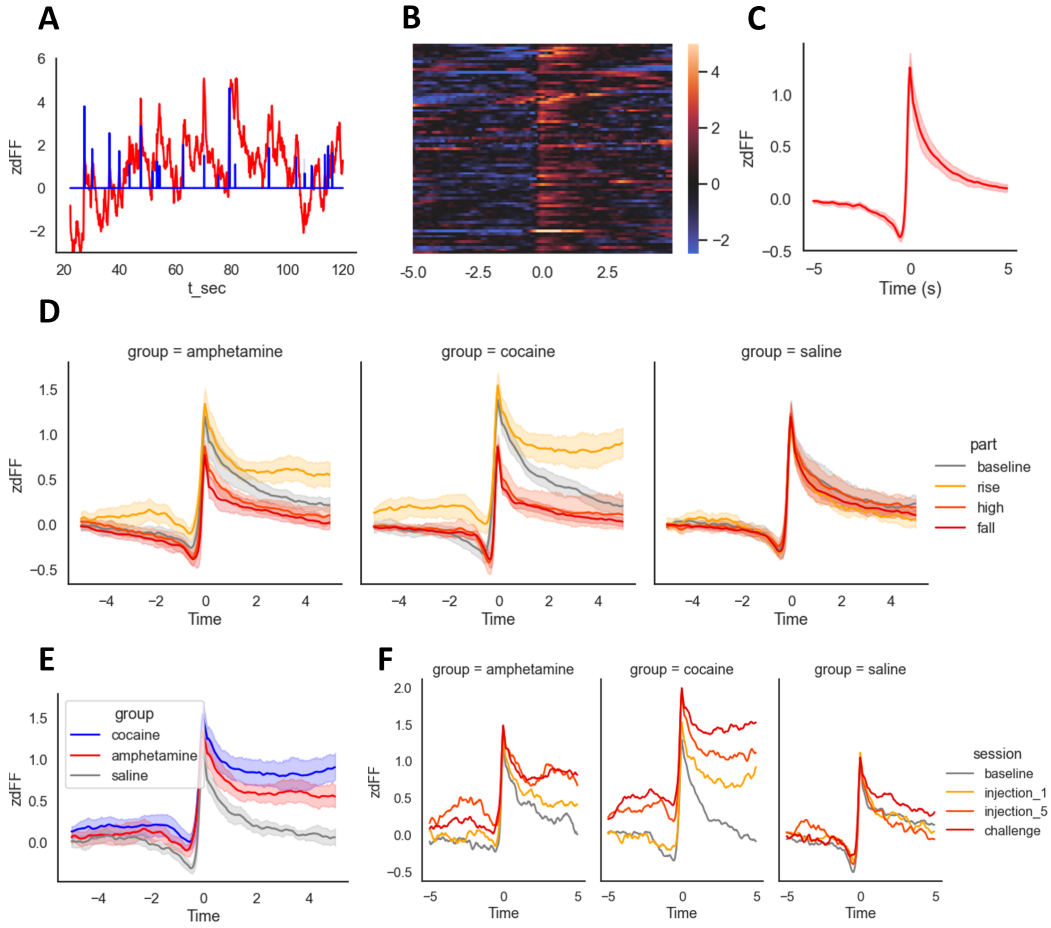

Figure 3.3: Dopamine Transients during Sensitization

A Dopamine trace (red) of representative animal and detected transients with size (blue) **B** Peri-events of the same mouse around dopamine transients > 1.5 z-scores, t = 0 is aligned to the maximum amplitude of the transient **C** Averaged dopamine traces for the baseline session of all mice around transients > 1 z-score **D** Averaged dopamine traces around dopamine transients separated by group and colored by the time when the transient was recorded (baseline: before injection; rise: 0-5 min after injection, high: 5-20 min after injection, fall: 20-50 min after injection). Only injections 1 and 5 are included because only there, saline animals received saline and the others the psychostimulant **E** Averaged dopamine traces around dopamine transients during "rise" (0-5 min after injection), colored by group **F** Same as D, but only for transients during "rise" (0-3 min after injection) and colored by session

assign a suited vertical and horizontal threshold, the basis of this algorithm. It also often fails to detect the onset of a transient and instead labels short outliers during the decay falsely as transients.

Second, other researchers used more advanced algorithms to match transients to a given shape. This works well under the assumption of a specific shape of the transients. Here, however, we cannot assume that transients after cocaine or amphetamine injection follow the same shape. Because cocaine and amphetamine block dopamine reuptake transporters, transients decay slower. That's why we chose an approach that focuses on the sharp rise. We smoothed the photometry data with a 300 ms moving average and defined transients as sharp, monotonically increasing sequences that are at least one z-score in size. This algorithm robustly yields the time of the maximum dopamine levels directly after a sharp rise (Figure 3.3 **A**). The algorithm also yields the size of the transient. We found that individual transients can have very different forms and shapes (Figure 3.3**B**), but the average is marked by a sharp rise and a long, exponentially decreasing decay (Figure 3.3**C**).

Cocaine blocks the dopamine reuptake transporter (DAT) which leads to a slower dopamine clearance from the extracellular space. We thus hypothesized that dopamine transients would decay slower. In addition, it has been shown that dopamine neurons are inhibited via D2 autoreceptors. Together with our prior findings about reduced fluctuation, we predicted that transients are smaller in amplitude. To compare transients, we divided each session into four parts: "baseline" for transients that occurred during the 10-minute baseline before injection; "rise" for 0 - 5 minutes after injection; "high" for 5 - 20 minutes after the injection"; and "fall" for transients 20 - 50 minutes after injection (Figure 3.3**D**). We observed that the amplitude of transients during "rise" is similar to baseline. However, dopamine decays less after a transient, suggesting that dopamine increases in an almost step-like fashion (Figure3.3**D**, middle panel). This is consistent with our neurobiology-inspired hypothesis. For "high" and "fall", dopamine transients also decay slower, but are also smaller in size, compared to rise or baseline.

Amphetamine acts via different mechanisms. While it also blocks DAT through competitive inhibition, it can also internalize or reverse DAT. This process is independent of activity and would produce a continuous dopamine efflux. We thought that these differences might be visible and hypothesized that dopamine would increase continuously, and not only after transients. However, we found that dopamine transients look similar compared to cocaine (Figure 3.3 **D**, left panel). We compared transients during the first 5 minutes after injection between groups (Figure 3.3**E**) and concluded that transients look similar for cocaine and amphetamine. However, transients after amphetamine injection decay slightly faster, an observation that is likely the result of the slower pharmacodynamics of amphetamine.

Lastly, we tested if phasic transients also sensitize. Because we observed that dopamine rises faster in sensitized mice earlier, we looked at the period of 0 - 3 minutes after injection specifically. We observe an increase in persistence during sensitization, meaning that transients decay slower in sensitized mice (Figure 3.3**F**).

In total, we extracted dopamine transients and showed that for both amphetamine and cocaine, transients decay slower and that this effect strengthens as the mouse gets sensitized.

3.4 Accumbal ACh levels and dynamics change in response to psychostimulants

We investigated how ACh changes in response to psychostimulants and during sensitization. To record extracellular ACh dynamics, we expressed an ACh sensor (GRAB-ACh3.0) together with the dopamine sensor (GRAB-rDA). This allowed us to capture ACh and dopamine simultaneously. In the Nucleus Accumbens Shell, ACh levels are stable, with short and sharp transients that occur irregularly at a frequency of 1-2 Hz (Figure 3.4**A**). These transients are likely the result of the synchronous firing of a population of cholinergic interneurons. Because we observed that baseline levels appear to be stable, we primarily analyzed these ACh events. We captured events by applying a simple filter that finds local maxima with a threshold of 2 z-scores (Figure 3.4**A**). We set the threshold to 2 z-scores as this threshold has been used and verified by other researchers using the same sensor [40].

We found that events are stereotypically short, sharp, and high in amplitude (Figure 3.4**B**). Looking at individual traces, we saw an apparent increase in amplitude after the injection of psychostimulants (Figure 3.4**C**). We investigated event-time data as frequencies via a 30-second moving window. We observed slight variations in the baseline frequency of detected events between animals that might be due to differences in expression. To compare and average, we calculated a baseline frequency per session using the first 10 minutes and subtracted the baseline from the frequency data. We observed a rapid and strong decrease in frequency after injection of amphetamine or cocaine, but not after saline (Figure 3.4**D, E**). A repeated measures ANOVA with the session as repeated measure and group as between-subject variable yielded a significant main effect for both (group: $F=6.757$, $p=0.0139$; session: $F=6.295$, $p=0.00192$) and a significant interaction ($F=6.234$, $p=0.000246$). We observed that the difference increased during sensitization for some animals (Figure 3.4**F**), but not for all. Thus, posthoc t-tests showed big differences between saline and psychostimulants during injection 5 (saline-cocaine: $p=0.00133$, saline-amphetamine: $p=0.00293$, amphetamine-cocaine: $p=0.382$, independent student's t-test), but not during the challenge, where animals of the saline group received either cocaine or amphetamine (saline-cocaine: $p=0.113$, saline-amphetamine: $p=0.0173$, amphetamine-cocaine: $p=0.466$).

We further investigated whether not only the number but also the amplitude of transients decreased. We extracted ACh traces around events, averaged them (Figure 3.4**G**), and found that their amplitude decreases after injection of cocaine or amphetamine (Figure 3.4**H**). A repeated measures ANOVA with the group as a between-subjects factor showed significant main effects for group ($F=16.88$, $p=0.000900$) and session ($F=17.24$, $p=0.000002$) and an interaction ($F=4.1$, $p=0.00470$). A posthoc test between groups at challenge injection also yielded a significant difference between saline and cocaine (saline-cocaine: $p=0.0423$, saline-amphetamine: $p=0.0870$, cocaine-amphetamine: $p=0.832$, independent student's t-test), suggesting that there is a sensitization effect.

We showed that after injection of cocaine and amphetamine, ACh events decrease in amplitude and frequency. Because we measure events with a fixed threshold, it's possible that not the real frequency decreases, but simply the amplitude and that subsequently, fewer events exceed the threshold. In that case, our estimate for the decrease in amplitude

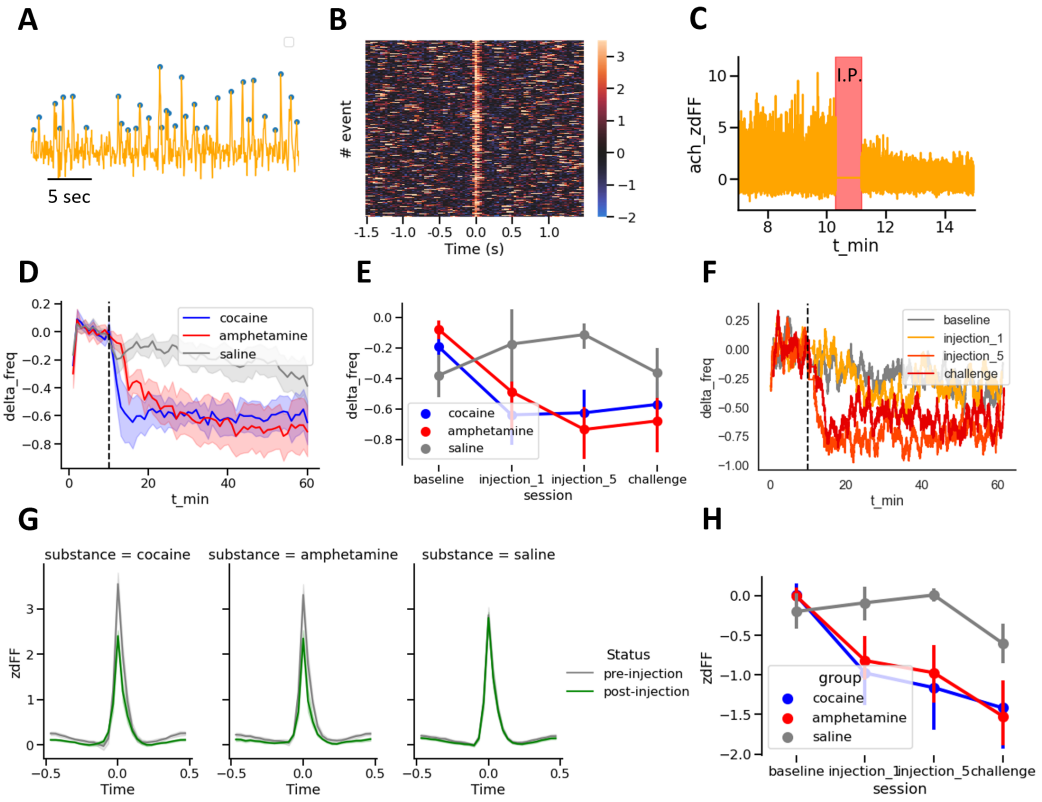

Figure 3.4: ACh Events decrease during Sensitization

A ACh trace of a representative animal with markers for detected events **B** Peri-events of the same mouse showing that ACh events are short and consistent transients **C** ACh trace around a cocaine injection of a representative animal **D** Averaged traces of difference between mean baseline frequency and event frequency around a 30-second moving window **E** Same measure as in D but aggregated for session and group **F** Same measure for a representative animal and all four sessions **G** ACh traces aligned to events by substance (all sessions where saline was given, for example also the baseline recording for all animals, is included, and so on). Grey shows averaged transients that occurred during the 10-minute baseline before injection, and green covers the 50 minutes after injection. **H** Quantification of G. For every session, the difference between peak height during the baseline and post-injection is calculated and shown. All error bars present the .95 confidence interval of mean, calculated by bootstrapping with 1000 iterations.

is a gross underestimate and could be much bigger. Furthermore, it could technically be the case that the observed sensitization effect is not only due to a decrease in amplitude after injection, but additionally to an increase before injection. This possibility is discussed in a later chapter.

3.5 Interaction between dopamine, ACh, and locomotion

After we looked at locomotion, dopamine, and ACh individually, we wanted to understand better how they relate - and how their relationship changes in response to psychostimulants. We systematically extracted dopamine, ACh, and locomotor activity traces and aligned them to dopamine transients, ACh events, and movement onset. This yielded a matrix that describes how locomotion, dopamine, and ACh correlate and how their correlation changes in response to cocaine and amphetamine.

First we looked at dopamine (Figure 3.5, first column). To detect dopamine transients, we used the method described earlier. Briefly, we defined transients as sharp, monotonically increasing sequences that are at least 1 z-score in height. Dopamine data aligned to transients yielded the average dopamine transient itself and is characterized by a sharp increase and slower, exponential decay. Here, transients after amphetamine or cocaine injection look similar to saline, but this is a mere artifact because transients that occur in the first few minutes are big and long whereas later transients are smaller in size (as shown in Figure 3.3). These two opposing characteristics lead to the fact that averaged dopamine transients after psychostimulant injection look similar to baseline transients.

We then aligned ACh data to the same transients and found that often, ACh transients cooccur with dopamine and reach their amplitude 0.2-0.6 seconds before the amplitude of a dopamine transient. It is important to note that there is no ACh transient before every rise in dopamine - however, cooccurrence is more probable than by chance. Cholinergic interneurons in the nucleus accumbens strongly modulate dopamine release via nicotinic receptors on dopamine neurons and can explain this observation. ACh spikes in photometry are thought to reflect synchroneity of cholinergic interneurons because the optic fiber is thick enough to cover (and thus measure) ACh release of a population of cholinergic interneurons. It has been shown that this synchronous ACh release amplifies dopamine transients [17]. We observe that the ACh transient is followed by a short pause which develops because dopamine transiently inhibits cholinergic interneurons by acting on their D2 receptors [41]. Because dopamine transients get smaller in amplitude as well after injection of amphetamine or cocaine, we found that the proportion between the size of dopamine and acetylcholine transients does not change (not shown).

Baseline movement does not correlate with dopamine release (Figure 3.5 first column, 3rd, and 4th plot). This is consistent with extensive prior literature that suggests that dopamine is related to movement in the dorsal striatum, but not the nucleus accumbens. Dopamine transients there are caused by reward prediction errors [1] but can correlate with movement if the information causing the prediction error makes movement necessary. Here, we observe that speed measured at the nose or at the base of the tail is increased sharply around dopamine transients only after injection of a psychostimulant.

Second, we extracted ACh events. Spikes occur at a frequency of 1-2 Hz but the time between two transients is unregular (see flat lines at the edges of the graph). We further

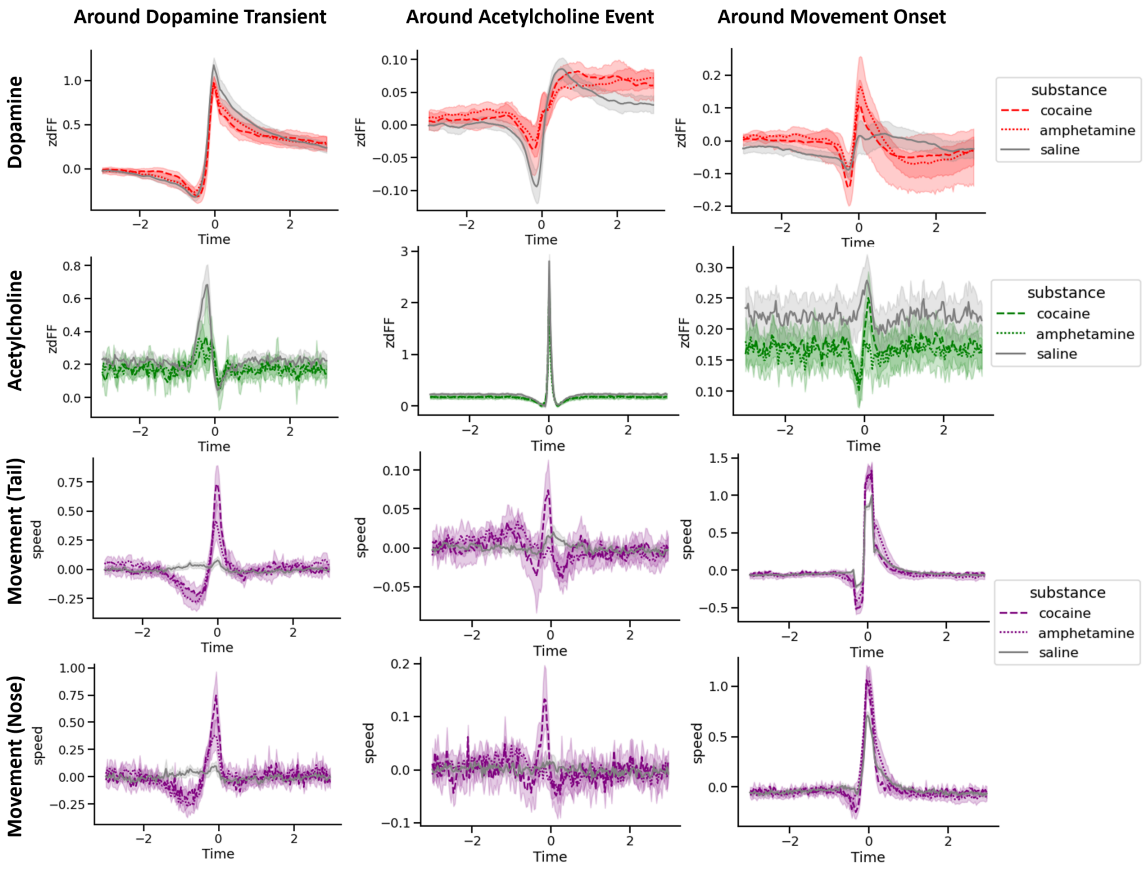

Figure 3.5: Correlations between dopamine, ACh, and locomotion

Graphs show averaged dopamine, ACh, and locomotor activity traces split by color in cocaine, amphetamine, and saline. All transients from a single session are averaged first. Then, a grand average across sessions is calculated. Error bars are calculated based on the session averages and represent the .95 confidence intervals of the mean based on bootstrapping with 1000 iterations. **First Column** All traces in the first column are aligned to the maximum amplitude of dopamine transients. Transients were extracted as described earlier. For example, the first plot shows dopamine traces around dopamine transients, the second plot shows ACh traces around the same dopamine transients, etc... **Second Column** All traces in the second column are aligned to ACh events. Events were extracted as described earlier **Third Column** All traces in the third column are aligned to the onset of locomotion. The base of the tail was the marker used to determine locomotion. The derivative was calculated to get positive acceleration. Then, we selected all local maxima above a threshold as the onset of movement.

observe that ACh transients are also related to dopamine; on average, there is an increase in dopamine after an ACh event. Also, dopamine decreases before an ACh event.

Similar to dopamine, ACh spikes are related to movement in the dorsal striatum [23] and are spike when movement has to be initiated or changed. In the ventral striatum, no such relationship is reported. Here, we also see no relationship to dopamine during baseline recordings. However, this changes after injection of cocaine, as there is a slight increase of speed close to ACh spikes. Although amphetamine seems to resemble the same pattern, this observation is much stronger in animals injected with cocaine.

Lastly, we extracted the onset of locomotor activity. We calculated the gradient of speed measured at the base of the tail to get acceleration. We then defined movement onset as positive, local maxima above a low threshold. Similar to our previous observations, we see that there is only a small relationship between dopamine and acetylcholine release that gets stronger after the injection of a psychostimulant.

Conclusively, we systematically compared the interaction between dopamine, acetylcholine, and locomotor activity. We reproduced findings from previous studies showing that dopamine transients sometimes occur in temporal succession of one (or several) ACh transients and confirmed that the correlation between both transmitters and movement is low initially. Interestingly, the administration of amphetamine or cocaine changes this relationship significantly.

3.6 Baseline Acetylcholine predicts Sensitization

The function of ACh is still a controversy. While electrophysiological research has primarily focussed on the cholinergic pauses, population recordings with optical sensors show a constant baseline with frequently occurring fast and sharp transients that are likely the result of synchronous firing. Synchronous firing is difficult to observe with electrophysiology, because cholinergic neurons are sparse and often, it's only possible to record from individual neurons. That might be a reason why more research was contributed to pauses in firing.

Most experiments only look at activity time-locked to certain external stimuli and cues. Here, we investigated, how dopamine relates to acetylcholine in general, not time-locked to specific external events. The following only provides correlative evidence and aims at identifying possible questions to test for. First, we were interested in how phasic dopamine activity relates to ACh. We averaged ACh traces time-locked to peaks of dopamine transients (Figure 3.6**A**). ACh is on average higher a few hundred milliseconds before a dopamine peak. Then, at the peak itself, we observe a decrease compared to baseline which could be interpreted as a cholinergic pause. Importantly, there is no ACh event before every dopamine transient but ACh events co-occur with dopamine transients more often than by chance (Figure 3.6**A, B**). This strengthens the idea that cholinergic firing can provoke or amplify dopamine release by acting on the nicotinic receptors on dopamine neurons. We thus asked, whether bigger dopamine transients are more often accompanied by ACh events. We again calculated the average of ACh traces around dopamine transients (Figure 3.6**B**) but this time split by the amplitude of the dopamine transient. We observed that the average ACh amplitude before a dopamine transient that is bigger than 4 z-scores is about 3 times as high compared to ACh traces around smaller

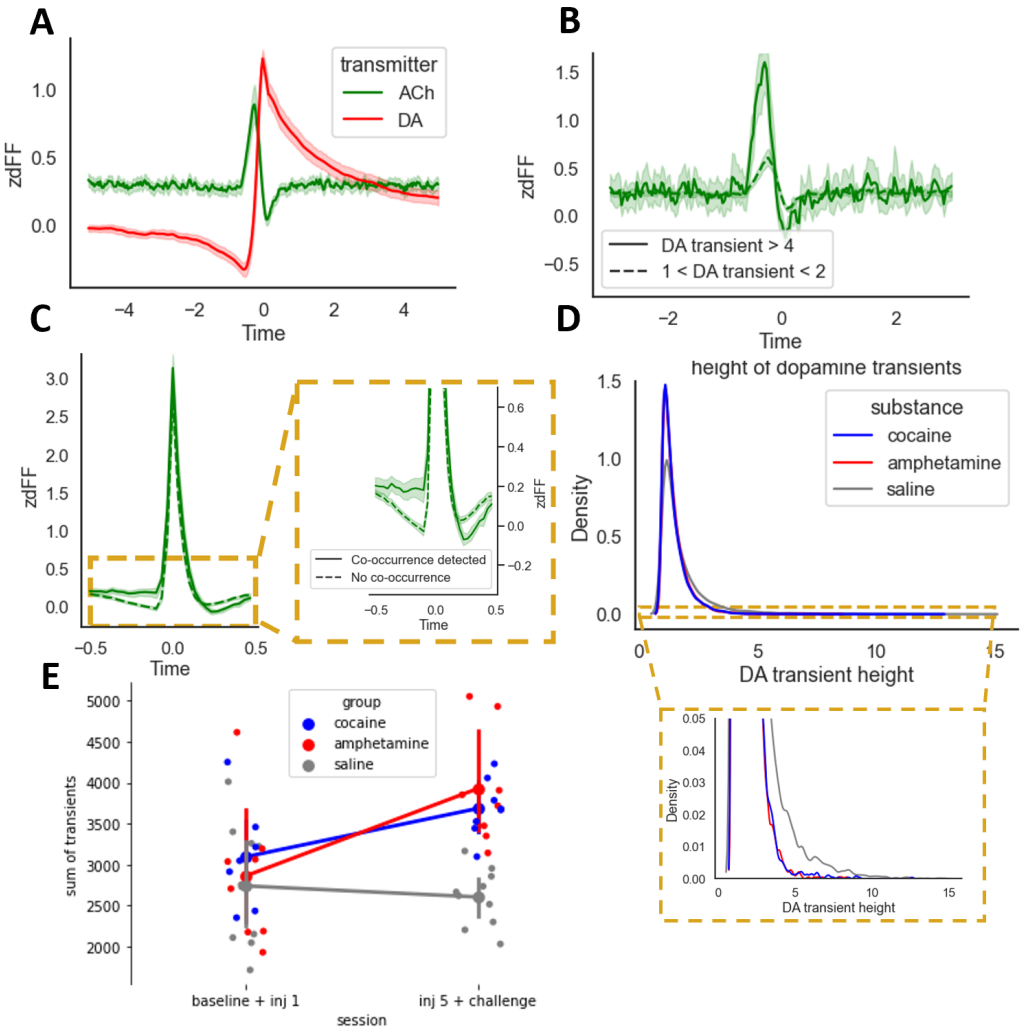

Figure 3.6: Baseline Acetylcholine predicts Sensitization

A Recorded dopamine and ACh data averaged around the peak time of dopamine transients **B** Averaged ACh data time-locked to dopamine transients and split by size of dopamine transients **C** Averaged ACh data time-locked to ACh events and split by whether a dopamine transient co-occurred within .8 seconds after the spike. Right panel zooms into the red rectangle of the left panel **D** Kernel density estimate for dopamine transients split by substance that was injected during the session. Kernel density estimates visualize the distribution of heights of dopamine transients. Lower panel zooms into the red rectangle of the upper panel **E** Baseline ACh predicts sensitization. Only data during the 10-minute baseline before injection was used for this analysis. Per session, the height of all detected ACh transients was summed. During baseline and injection 1, no animal had prior exposure to psychostimulants. For injection 5 and challenge, animals of the amphetamine and cocaine, but not the saline group had prior exposure to psychostimulants. All error bars present the .95 confidence interval for the mean measured by bootstrapping with 1000 iterations

dopamine transients between 1 and 2 z-scores, suggesting that ACh amplitude modulates dopamine amplitude.

We were also interested in whether dopamine transients predict the cholinergic pause. This time, we looked at ACh events and determined events that were followed by a dopamine transient 200-800 ms after peak of the transient. Again, we looked at ACh traces and observed that the decrease after an ACh event in ACh is bigger if a dopamine transient occurred shortly after the ACh event. Although only correlational, it supports the idea that high dopamine concentration inhibits cholinergic interneurons via their D2 receptors. Interestingly, we also observe a difference before the ACh peak. For a typical ACh peak, fluorescence is decreased around the transient itself, which indicates that it is less likely that two events occur in very close succession which is biologically plausible. However, before an event that was followed by a dopamine transient, we didn't see this effect which suggests that an ACh event that is related to a dopamine transient is independent of other ACh events. This could possibly be because both react to a specific stimuli or event but this is speculative (Figure 3.6**C**).

Because of our observation that bigger dopamine transients are accompanied by bigger ACh transients and because ACh transients decrease in size when exposed to cocaine or amphetamine, we investigated whether dopamine transients are smaller after the injection of cocaine or amphetamine when ACh events are smaller as reported earlier. We calculated the Kernel Density Estimate and observed that the ratio of small vs big transients is indeed tilted towards smaller transients after exposed to a psychostimulant (Figure 3.6**D**).

Lastly, we investigated whether ACh firing is different in sensitized mice before injection with a psychostimulant. Multiple studies suggest that ACh is needed in some form to associate cues with rewards. For example, it has been shown that cue-evoked cholinergic pauses are needed for associating cues, or that a lower ACh event rate correlates to a lower degree of cocaine extinction. This correlation could implicate that pauses are longer and longer pauses implicate greater association. However, it could also be the case that ACh events are needed to induce synaptic plasticity and that because of this, animals with lower frequencies extinguish less.

We tried to find a measure that accounts for both the event frequency and the amplitude and simply took the sum of peak z-score for every ACh event that happened during the 10-minute baseline before injection. We split the data into two groups: We aggregated baseline and injection 1, because here, none of the animals had pre-exposure to any psychostimulant. Then, we aggregated sessions from injection 5 and challenge, because here, animals of the amphetamine or cocaine group had prior exposure but not animals of the saline group. We summed peak z-scores of ACh events seperately per session. We found that ACh is significantly increased only for the animals that had prior exposure to psychostimulants (Figure 3.6**E**). A repeated measures ANOVA with session as repeated measure and group as between-subject factor revealed a significant main effect of session ($F = 21.8$, $p = 0.000881$) and a significant interaction between group and session ($F = 12.99$, $p = 0.00167$). Post hoc pairwise t-tests showed no significant difference between groups during baseline and injection 1 (cocaine-saline: $p = 0.24$, amphetamine-saline: $p = 0.77$, amphetamine-cocaine: $p = 0.56$) but significant differences between drugs and saline for injection 5 and challenge (cocaine-saline: $p = 0.00388$, amphetamine-saline: $p = 0.342$, amphetamine-cocaine: $p = 0.565$).

Conclusively, we observed a close relationship between dopamine and acetylcholine and a possibly interesting effect of higher ACh release after exposure to psychostimulants. Although all evidence presented is correlative and conclusions remain speculation, it shows interesting interaction effects that should be investigated closer in future experiments.

3.7 MoSeq allows for precise quantification of behavior and describes behavioral sensitization better

So far, we only investigated population effects. Per group, we averaged individual animals together to find differences between groups. However, mice and humans sensitize to drugs differently and it is of great importance to find causes and investigate which factors, circuits, and receptors contribute how to the effect of psychostimulant sensitization. With our data, for example, we might seek to quantify the exact relationship between dopamine, acetylcholine, and behavior. There are a variety of open questions. Is the behavior after the first injection a predictor of sensitization? Or does the increase in dopamine or the amount of ACh predict behavioral sensitization in later sessions? Do drug-induced behavioral changes rise and fall in an exact relationship to dopamine?

These questions are difficult to answer because the locomotor activity is a very noisy measurement of the underlying behavioral sensitization. Dopamine evoked by psychostimulants affects different parts of the brain, mainly the prefrontal cortex and the ventral and dorsal striatum. These regions are not only responsible for initiating locomotor activity, but also for planning, goal-directed behavior, compulsion, cognitive control, action selection, or associating cues with rewards. Thus, the increase in locomotion is not the primary result of the injection of cocaine or amphetamine. Instead, it is a side effect of the underlying sensitization - a process that leads to behavioral changes that get stronger after multiple exposures to psychostimulants.

We investigated two individual mice of the cocaine group. For the first mouse (Figure 3.7**A-C**), we observed that locomotor activity was increased during injection 5 and challenge for the first minutes compared to the first injection of cocaine (Figure 3.7**A**). Then, however, movement decreased and was lower compared to the first injection. Yet, the dopamine data showed normal behavior and stayed consistently high and exceeded the dopamine levels of the first injection even during periods of little movement (Figure 3.7**B**). A manual analysis of the video showed that this mouse exhibited repetitive behaviors that were low in locomotion. For example, it was often facing toward the wall of the open-field arena and repetitively touching or staring at it (Figure 3.7**C**). Repetitive behaviors are a clear symptom of psychostimulants and psychostimulant-induced sensitization, but decrease the amount of locomotion. We conclude that for this animal, locomotion is an inaccurate measure of behavioral sensitization.

We investigated a second mouse that showed high amounts of irregularities in locomotion (Figure 3.7**D-F**). During injection 5 and the challenge, locomotor activity was extremely elevated compared to other mice during the first 15-20 minutes after injection. Then, it suddenly dropped to levels below the baseline and stayed low except for short bouts of fast movement (Figure 3.7**D**). Dopamine was slightly increased compared to the first cocaine injection and in contrast to locomotion, it was consistently high and smooth (Figure 3.7**E**). Again, we investigated the video and found that this mouse was grooming

excessively during bouts of low locomotion (Figure 3.7**F**). Excessive grooming is also known to occur after injection of psychostimulants but is not covered by our measurement. Strikingly, excessive grooming affects our measurement negatively because locomotor activity can drop below baseline levels and could lead to the wrong conclusion, that this animal did not sensitize.

Both animals show that it is necessary to develop better and more robust measurements of the behavioral effects of sensitization. Here, we trained a model that densely labels behavior using MoSeq. MoSeq is a method to cluster 3D video data of mice into behavioral syllables using an unsupervised approach. We captured 3D point clouds using a Microsoft Kinect (Figure 3.7**G**) and extracted and aligned the mouse with a pre-trained model such that the nose of the mouse always points to the right (Figure 3.7**H**). We extracted the first 30 minutes after injection. Then, we performed an iterative PCA to reduce dimensionalities (Figure 3.7**I**). We found that the top 5 principal components explain more than 90 % of the variance and we selected 10 principle components for further modeling. We then trained an autoregressive hidden Markov model (Figure 3.7**J**) to cluster the video data. Hidden Markov models are statistical sequence models that were originally developed for natural language processing but are now applied in many other fields. Hidden Markov models model the full joint distribution of hidden and observable states and are thus generative. The model learns to cluster behavior into a limited set of behavioral "syllables" that are each between 200 and 400 ms long and describe a stereotypical behavior (Figure 3.7**K**).

The AR-HMM clustered the behavior into 72 individual syllables, out of which we omitted 11 syllables that together had a usage of less than 1 %. First, we calculated the transition matrices between syllables separately for sessions where different substances were injected (Figure 3.8**A**). A transition matrix shows the probability of syllable B occurring next given syllable A. Concretely, we calculated the transition matrix for all sessions where saline was injected, e.g. the baselines for every animal, but not the challenge injection of the saline group as these animals also received psychostimulants for the challenge injection. For saline, we saw that the transition matrix is sparse but that most syllables have multiple successors with a high probability. In contrast to this, we observed that the transition matrixes for cocaine and amphetamine are much more sparse. This means, for many syllables, only one or a few syllables have a high probability of succession. Thus, the behavior of these mice is more predictable.

Now, we wanted to know whether these syllables carry a human-understandable meaning and what exactly these changes are in terms of behavior. We manually investigated each syllable to determine whether the syllable consistently represents a concrete behavior. For each syllable, we extracted 12 occurrences of that syllable. We extracted a 3-second video around the onset of each occurrence. We then produced an overlay that showed the video for all occurrences simultaneously (Figure 3.8**B**).

Most of the syllables denoted a specific motor movement. Most strikingly, motor movements where the mouse changed in height were clustered best, because this data is clear and sharp as we used depth videos. Different syllables were used for individual parts or rears, for example, rears of different heights were separated into different syllables. Also, different phases of a rear such as "rear up", "maintain rear", "rear and rotate" or "rear down" were separated. Furthermore, many other motor movements were detected (Figure 3.8**B, C**). These include clockwise and counter-clockwise fast movements, light and sharp turns, and different kinds of freezing or states without motor movement.

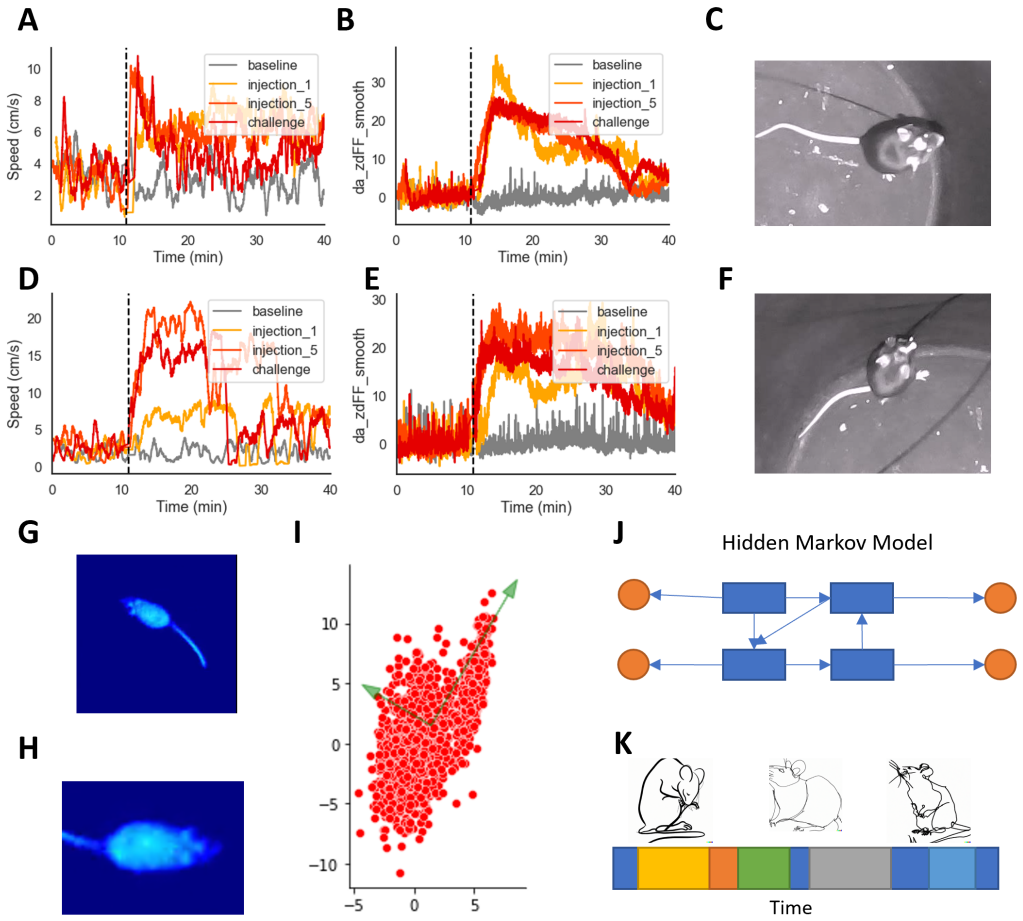

Figure 3.7: Motivation and Integration of MoSeq

A-F Rational for using MoSeq: Why are better behavioral measurements needed? **A** Locomotor activity of a representative animal split by session and measured at the base of the tail. During injection 5 and challenge, locomotor activity drops below the level of the first injection although dopamine levels stay consistently high **B**. **C** Instead of running, the animal shows repetitive behaviors, for example touching and staring at the walls of the open-field arena. **D-F** Same as A-C, but of another animal. This animal shows excessive and repetitive grooming instead of running **G-K** Overview of the MoSeq pipeline **G** Depth video after background subtraction **H** A pre-trained classifier crops the mouse and aligns it such that the tip of the nose is on the right and the tail on the left **I** Then, PCA is performed to reduce dimensionality. The scatterplot is an illustration of PCA: PCA converts the data into a new coordinate system such that the axes minimize the average squared distance from the axis. The first 10 principal components explain more than 90 % of the variance and are used for modeling **J** Conceptual illustration of a Hidden Markov Model (HMM). Blue rectangles denote hidden states, orange circles the observable syllables. The HMM is trained in an autoregressive unsupervised manner to cluster the video data into less than 100 syllables. Detected syllables are 200-400 ms long **K** Illustration of the output of the model. After training, the model performs inference on all experimental data to extract a long sequence of syllables for every animal

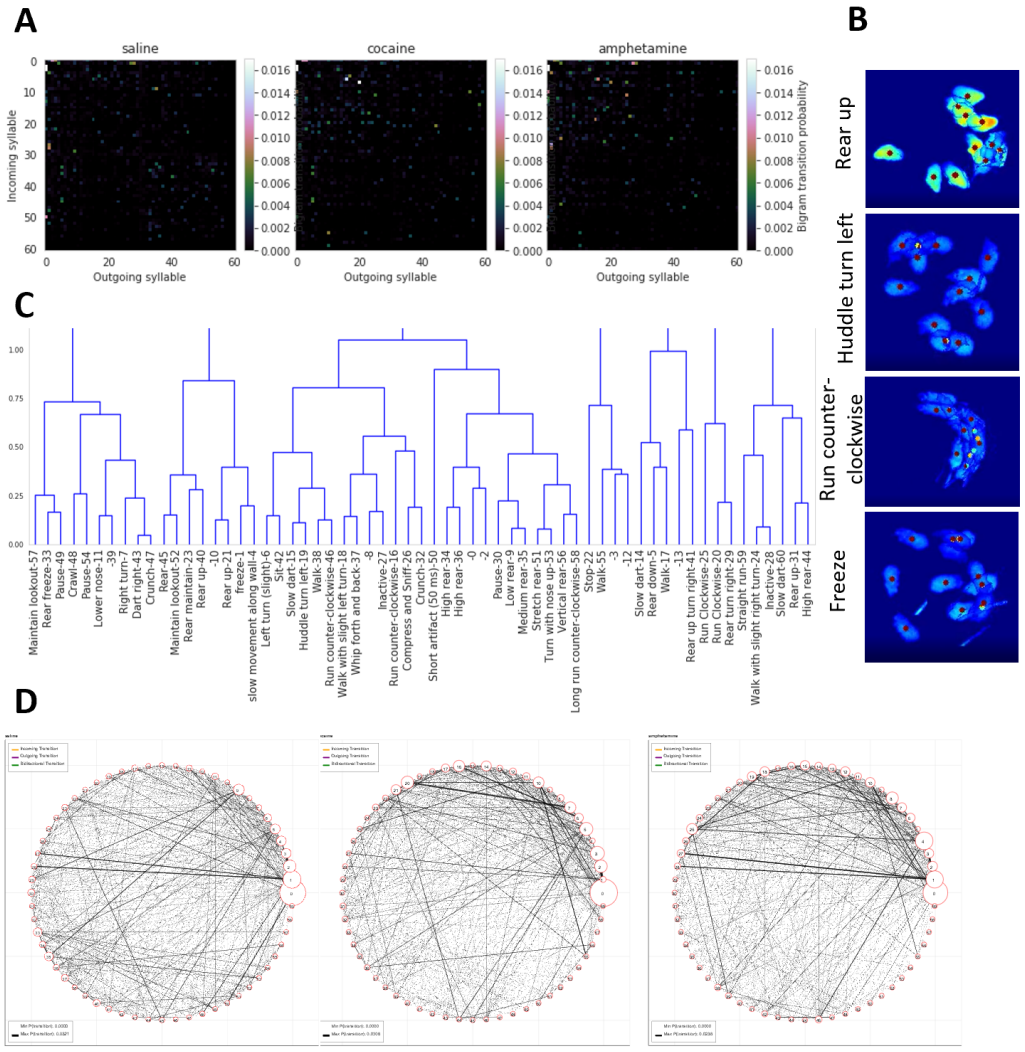

Figure 3.8: Evaluation of the MoSeq Model

A Transition matrix for animals that received saline, cocaine, or amphetamine, respectively. Color denotes the probability of transition from one to the other syllable **B** Overlay of 12 animals while they perform the same syllable. Syllables are 200-400 ms long, and it's not possible to present video data here. However, the screenshots give an impression of what the respective syllable describes **C** Syllable dendrogram. It represents the hierarchically sorted pairwise distances between the model's autoregressive matrices. Each syllable was manually reviewed and a fitting title for that syllable was selected **D** Syllable graph for amphetamine, saline, and cocaine, respectively. Every circle represents a syllable, and its size is the syllable usage. The thickness of each line shows a transition probability between two respective syllables.

We observed that some syllables appear to be similar, such as high rears and normal rears, or different kinds of freezing. Thus, we investigated whether these syllables are also similar in the space of the AR-HMM. Showing this would make it possible to compress the big number of syllables into less, more expressive ones and would also prove the precision of the model. We extracted the model's autoregressive matrices for each syllable, made a pairwise comparison, and sorted hierarchically. This yielded a dendrogram where syllables whose autoregressive matrix is most similar are clustered together (Figure 3.8**C**). We performed this step after manually giving a title to every syllable to see whether syllables labeled similarly by us also appeared together in the dendrogram. We found that this is actually the case. For example, the syllables labeled as "high rear" were closest together (Figure 3.8**C**). We further found that syllables close together often share common features, for example, speed ("Walk"(38), and "Run counter-clockwise"(46)), rotation ("Rear up turn right" (41), "Run clockwise" (25 and 20) and "Rear turn right"), height ("medium rear"(35), "low rear"(9), "stretch rear", "turn with the nose up"(53) and "vertical rear"(56)), and movement ("maintain lookout"(57), "rear freeze"(33), and "pause"(49") (Figure 3.8**C**).

Now, as we found that syllables carry specific meanings, we investigated which syllables and transitions changed after exposure to cocaine and amphetamine. We revisited the transition matrices and sought to identify which syllables and which transitions exactly were up or downregulated after treatment with psychostimulants. To better visualize changes, we plotted syllables in a circumferential way and altered the size to show syllable usage. We then draw lines between syllable transitions and altered the size of the line to show the probability of this transition (Figure 3.8**D**, suppl. Figures 5.7, 5.8, 5.9 for bigger illustration). We saw clear differences between treatments and sought to investigate differences closer.

We compared syllable usage and transitions between cocaine and saline (Figure 3.9), amphetamine and saline (Suppl. Figure 5.10, and amphetamine and cocaine (Suppl. Figure 5.11). We analyzed the differences between cocaine and saline in more depth. We see that many syllables and transitions that are upregulated after cocaine treatment are related to movement, for example, "run clockwise", "counter-clockwise", "right turn" or "approach wall". This is expected from our previous findings and shows that MoSeq can annotate data precisely and correctly. Interestingly, especially connections between movements are upregulated, for example after "right turn" often follows "run clockwise". This suggests that bouts of locomotor activity last longer and that mice treated with saline might occasionally run, but not consistently without breaking.

We then investigated which syllables are downregulated after cocaine treatment. Interestingly, we found that many syllables related to exploration are more often used after saline injection than cocaine. Syllables used more frequently are "nose up", "high rear", "medium-sized rear", and "rear freeze". This reproduces the well-known psychostimulant-induced reduction in exploratory behaviors. Besides these, syllables related to inactivity were less after cocaine injection as well. Regarding the transition probabilities, we observed that for cocaine, a small subset of transitions is heavily upregulated at the expense of downregulating most other transitions. This could indicate that behavior after the cocaine challenge is more predictable and less complex.

The evidence presented here is not conclusive. Our goal was to investigate whether MoSeq can be used to get better behavioral measurements that can be used to determine the amount of behavioral sensitization. Here, we showed that our model is able to cluster

the data into meaningful motor movements and that it can detect differences in locomotor activity and exploratory behavior. It is up for future work to use this dataset to investigate how it can help to quantify the degree of sensitization.

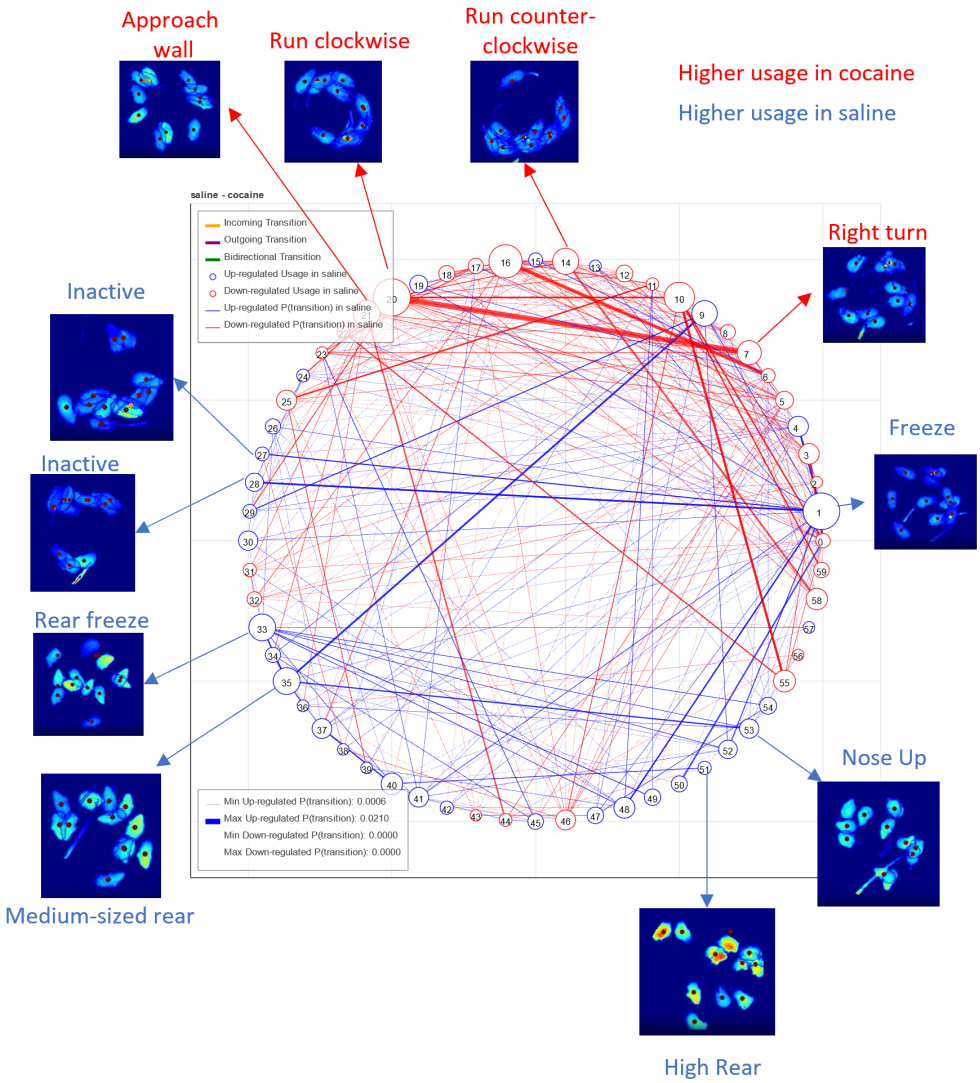

Figure 3.9: MoSeq identifies differences in locomotor activity and exploratory behavior
Shown is a transition graph that shows the differences between cocaine and saline. Red shows higher usage of a syllable after cocaine injection, and blue shows higher usage of a syllable after saline injection compared to dopamine. The size of the circles and transition lines denote the size of the difference for syllable usage and syllable transition probability, respectively. For the biggest differences, screenshots of mice performing the indicated syllable are shown

4 Discussion and Future work

We built a densely annotated dataset of 63 sessions of 60 minutes. We recorded dopamine and acetylcholine in the nucleus accumbens shell and extracted transients for both transmitters. Simultaneous to neural measurements, we recorded a video and trained a Computer Vision model with DeepLabCut to programmatically annotate 13 different markers on the mice's bodies. In addition, we collected 3D data of the mouse pose and used MoSeq to annotate all data with specific behavioral syllables. We hope that this dense dataset of behavior, neural data, and manipulation through repeated injection of psychostimulants will be interesting for future analyses. In addition to experiments shown here, we later subjected the same animals to a battery of operand conditioning tests (not shown here) to allow for potentially interesting post hoc within-animal analyses that combine sensitization with conditioning.

Using a dopamine-insensitive version of the genetically encoded transmitter indicator, we were able to develop and verify a method to remove photobleaching and artifacts from the raw data despite the drug-induced tonic increase in dopamine that happened at a similar frequency to photobleaching. We then characterized the effects of drug-induced sensitization on dopamine on different time scales. We showed that in sensitized mice dopamine amplitude increases, rises faster upwards after injection, fluctuates less, has fewer transients, and those transients also change in size and decay. This analysis on different timescales highlights the interaction between what was formerly considered completely separate "phasic" and "tonic" firing modes. In many paradigms, for example in operand conditioning, phasic dopamine transients are aligned to a baseline taken a few seconds before each trial. This method removes information about the absolute dopamine concentration completely. In other experiments not discussed here, we observed dopamine ramps before predictable food rewards that were several minutes long and can potentially influence the amplitude of phasic transients in response to the reward. Thus, we argue that photometry data can and should be used to look at dopamine at different timescales, even if the primary goal is to only identify how the amplitude of transients changes.

We used dual-color photometry to record acetylcholine dynamics simultaneously to dopamine. We observed that amplitude and frequency of ACh events decreased after an injection of cocaine or amphetamine and that the decrease in amplitude gets stronger with sensitization. This shows the close dopamine-acetylcholine interaction in the nucleus accumbens. However, what we could not observe is whether the overall acetylcholine concentration increased or decreased. While it seems easy to argue that concentration goes down with decreasing number of ACh events, it is also possible that the tonic concentration rises and that the smaller amplitude of transients is due to a ceiling effect.

In a systematic way, we extracted dopamine, acetylcholine, and movement data that was time-locked to dopamine and acetylcholine transients, and onset of movement. We found that movement initially had no relationship to neural activity in nucleus accumbens shell which was expected as nucleus accumbens is primarily involved in rewards and not

in motor movements. However, we found that this changes in response to drugs and that most of these changes seem to get stronger with sensitization.

Although locomotor activity is a strong measure of the behavioral effect of a psychostimulant, it is by far not the only variable that changes a mouse's behavior. Besides locomotion, animals often show repetitive behaviors like excessive grooming and exploratory behavior decreases. We found that especially repetitive behaviors that are stationary negatively affect the measurement of behavioral sensitization, thus making locomotion a very noisy measurement of psychostimulant sensitization. However, it is difficult to measure the mouse's behavior holistically.

Grooming behavior is often manually annotated, either during the experiment or post hoc via a video recording. This process is slow and error-prone. There are a few commercial solutions that can automatically detect grooming, but these are still error-prone and need a video with good contrast between the mouse and the background. However, to not confound photometry recordings that operate in the visual spectrum, we need to record in the dark and use IR cameras. There, contrast is quite low and we found that established mouse trackers even fail to simply track the location of the mouse, even after manually tweaking all parameters. In addition, grooming is not the only behavior that mice perform in an excessive and repetitive way. We also observed that some mice approach the wall in a repetitive way and think that it is necessary to cover a wider range of behaviors to fully understand how behavior changes in response to repeated treatment with drugs of abuse. We argue that either MoSeq alone, or MoSeq together with DeepLabCut can provide deeper insights into repetitive behaviors because it can quantify the amount of the behavior of interest, but it also quantifies how "repetitive" behavior is by analyzing the sequence of syllables.

We investigated whether it is possible to detect sequences of excessive grooming using MoSeq. While it might be possible to do so, we think that this will be more difficult than detecting motor movements related to locomotion and exploratory behavior, because grooming looks similar to freezing, inactivity, or other behaviors that require no movement. However, it might be possible to use our annotations generated with DeepLabCut for this purpose. Position of the nose, eyes, ears, and paws are annotated and it might be possible to extract grooming behaviors with a simple threshold algorithm or to train a simple model with a very limited number of training samples.

Exploratory behavior is also reduced while exposed to drugs of abuse and is difficult to quantify. Traditionally, basic measures from open-field tests or mazes are used to quantify the amount of exploration. For example, the locomotor activity itself is often used as a proxy for exploration but would show a highly false result if used here. Another measure is the time that the mouse spends in the center of the open field, but this test can also be used to test for anxiety, similar to the elevated plus maze, and is thus not specific to exploration. Here, we showed that MoSeq can detect a whole range of different motor activities that are clearly related to exploration like rearing, sniffing, or rising the nose into the air. We also showed that exploratory behavior is decreased after the injection of cocaine.

Here, we tested MoSeq and developed a dataset of psychostimulant sensitization. Using these data to investigate behavioral changes during sensitization is content for future work.

Bibliography

[1] Wolfram Schultz, Peter Dayan, and P Read Montague. "A neural substrate of prediction and reward". In: *Science* 275.5306 (1997), pages 1593–1599.

[2] Scott J Russo, David M Dietz, Dani Dumitriu, John H Morrison, Robert C Malenka, and Eric J Nestler. "The addicted synapse: mechanisms of synaptic and structural plasticity in nucleus accumbens". In: *Trends in neurosciences* 33.6 (2010), pages 267–276.

[3] Eric J. Nestler. "Cellular basis of memory for addiction". In: *Dialogues in Clinical Neuroscience* 15.4 (2013). PMID: 24459410, pages 431–443. DOI: 10.31887/DCNS.2013.15.4/enestler. eprint: https://doi.org/10.31887/DCNS.2013.15.4/enestler. URL: https://doi.org/10.31887/DCNS.2013.15.4/enestler.

[4] Brooke N. Bender and Mary M. Torregrossa. "Molecular and circuit mechanisms regulating cocaine memory". In: *Cellular and molecular life sciences : CMLS* 77.19 (2020), pages 3745–3768. DOI: 10.1007/s00018-020-03498-8.

[5] Terry E. Robinson and Kent C. Berridge. "The neural basis of drug craving: An incentive-sensitization theory of addiction". In: *Brain Research Reviews* 18.3 (1993), pages 247–291. ISSN: 0165-0173. DOI: https://doi.org/10.1016/0165-0173(93)90013-P. URL: https://www.sciencedirect.com/science/article/pii/016501739390013P.

[6] "Zessen-Dynamic dichotomy of accumbal population activity underlies cocaine sensitization-2021-eLife". In: ().

[7] Erin S. Calipari, Rosemary C. Bagot, Immanuel Purushothaman, Thomas J. Davidson, Jordan T. Yorgason, Catherine J. Peña, Deena M. Walker, Stephen T. Pirpinias, Kevin G. Guise, Charu Ramakrishnan, Karl Deisseroth, and Eric J. Nestler. "In vivo imaging identifies temporal signature of D1 and D2 medium spiny neurons in cocaine reward". In: *Proceedings of the National Academy of Sciences of the United States of America* 113.10 (2016), pages 2726–2731. DOI: 10.1073/pnas.1521238113.

[8] Sebastiano Bariselli, Nanami L. Miyazaki, Meaghan C. Creed, and Alexxai V. Kravitz. "Orbitofrontal-striatal potentiation underlies cocaine-induced hyperactivity". In: *Nature communications* 11.1 (2020), page 3996. DOI: 10.1038/s41467-020-17763-8.

[9] Paul E. M. Phillips*†‡, Garret D. Stuber‡§, Michael L. A. V. Heien†, R. Mark Wightman†‡§ & Regina M. Carelli. "Subsecond dopamine release promotes cocaine seeking". In: *Nature* 422.6932 (2003), pages 611–614. DOI: 10.1038/nature01566.

[10] Chao Wei, Xiao Han, Danwei Weng, Qiru Feng, Xiangbing Qi, Jin Li, and Minmin Luo. "Response dynamics of midbrain dopamine neurons and serotonin neurons to heroin, nicotine, cocaine, and MDMA". In: *Cell discovery* 4.1 (2018), pages 1–16.

[11] Dan P. Covey, Mitchell F. Roitman, and Paul A. Garris. "Illicit dopamine transients: reconciling actions of abused drugs". In: *Trends in neurosciences* 37.4 (2014), pages 200–210. DOI: 10.1016/j.tins.2014.02.002.

[12] Joachim Brumberg, Sebastian Küsters, Ehab Al-Momani, Giorgio Marotta, Kelly P. Cosgrove, Christopher H. van Dyck, Ken Herrmann, György A. Homola, Gianni Pezzoli, Andreas K. Buck, Jens Volkmann, Samuel Samnick, and Ioannis U. Isaias. "Cholinergic activity and levodopa-induced dyskinesia: a multitracer molecular imaging study". In: *Annals of clinical and translational neurology* 4.9 (2017), pages 632–639. ISSN: 2328-9503. DOI: 10.1002/acn3.438.

[13] Ben D Bennett and Charles J Wilson. "Spontaneous activity of neostriatal cholinergic interneurons in vitro". In: *Journal of Neuroscience* 19.13 (1999), pages 5586–5596.

[14] Salah El Mestikawy, Åsa Wallén-Mackenzie, Guillaume M Fortin, Laurent Descarries, and Louis-Eric Trudeau. "From glutamate co-release to vesicular synergy: vesicular glutamate transporters". In: *Nature Reviews Neuroscience* 12.4 (2011), pages 204–216.

[15] Raad Nashmi and Henry A Lester. "CNS localization of neuronal nicotinic receptors". In: *Journal of Molecular Neuroscience* 30.1-2 (2006), pages 181–184.

[16] D James Surmeier, Jun Ding, Michelle Day, Zhongfeng Wang, and Weixing Shen. "D1 and D2 dopamine-receptor modulation of striatal glutamatergic signaling in striatal medium spiny neurons". In: *Trends in neurosciences* 30.5 (2007), pages 228–235.

[17] Sarah Threlfell, Tatjana Lalic, Nicola J Platt, Katie A Jennings, Karl Deisseroth, and Stephanie J Cragg. "Striatal dopamine release is triggered by synchronized activity in cholinergic interneurons". In: *Neuron* 75.1 (2012), pages 58–64.

[18] Volodymyr I Pidoplichko, Mariella DeBiasi, John T Williams, and John A Dani. "Nicotine activates and desensitizes midbrain dopamine neurons". In: *Nature* 390.6658 (1997), pages 401–404.

[19] Fu-Ming Zhou, Charles J Wilson, and John A Dani. "Cholinergic interneuron characteristics and nicotinic properties in the striatum". In: *Journal of neurobiology* 53.4 (2002), pages 590–605.

[20] Matthew T. C. Brown, Kelly R. Tan, Eoin C. O'Connor, Irina Nikonenko, Dominique Muller, and Christian Lüscher. "Ventral tegmental area GABA projections pause accumbal cholinergic interneurons to enhance associative learning". In: *Nature* 492.7429 (2012), pages 452–456. DOI: 10.1038/nature11657.

[21] Yan-Feng Zhang, John N. J. Reynolds, and Stephanie J. Cragg. "Pauses in Cholinergic Interneuron Activity Are Driven by Excitatory Input and Delayed Rectification, with Dopamine Modulation". In: *Neuron* 98.5 (2018), 918–925.e3. DOI: 10.1016/j.neuron.2018.04.027.

[22] John N. J. Reynolds, Riccardo Avvisati, Paul D. Dodson, Simon D. Fisher, Manfred J. Oswald, Jeffery R. Wickens, and Yan-Feng Zhang. "Coincidence of cholinergic pauses, dopaminergic activation and depolarisation of spiny projection neurons drives synaptic plasticity in the striatum". In: *Nature communications* 13.1 (2022), page 1296. DOI: 10.1038/s41467-022-28950-0.

[23] Mark Howe, Imane Ridouh, Anna Letizia Allegra Mascaro, Alyssa Larios, Maite Azcorra, and Daniel A Dombeck. "Coordination of rapid cholinergic and dopaminergic signaling in striatum during spontaneous movement". In: *Elife* 8 (2019), e44903.

[24] Jan M. Schulz and John N. J. Reynolds. "Pause and rebound: sensory control of cholinergic signaling in the striatum". In: *Trends in neurosciences* 36.1 (2013), pages 41–50. DOI: 10.1016/j.tins.2012.09.006.

[25] Huijeong Jeong, Annie Taylor, Joseph R Floeder, Martin Lohmann, Stefan Mihalas, Brenda Wu, Mingkang Zhou, Dennis A Burke, and Vijay Mohan K Namboodiri. "Mesolimbic dopamine release conveys causal associations". In: *Science* (2022), eabq6740.

[26] Korleki Akiti, Iku Tsutsui-Kimura, Yudi Xie, Alexander Mathis, Jeffrey Markowitz, Rockwell Anyoha, Sandeep Robert Datta, Mackenzie Weygandt Mathis, Naoshige Uchida, and Mitsuko Watabe-Uchida. *Striatal dopamine explains novelty-induced behavioral dynamics and individual variability in threat prediction*. 2021. DOI: 10.1101/2021.12.21.473723.

[27] Ilana B. Witten, Shih-Chun Lin, Matthew Brodsky, Rohit Prakash, Ilka Diester, Polina Anikeeva, Viviana Gradinaru, Charu Ramakrishnan, and Karl Deisseroth. "Cholinergic interneurons control local circuit activity and cocaine conditioning". In: *Science (New York, N.Y.)* 330.6011 (2010), pages 1677–1681. DOI: 10.1126/science.1193771.

[28] Zachary T Pennington, Zhe Dong, Yu Feng, Lauren M Vetere, Lucia Page-Harley, Tristan Shuman, and Denise J Cai. "ezTrack: An open-source video analysis pipeline for the investigation of animal behavior". In: *Scientific reports* 9.1 (2019), pages 1–11.

[29] Alfonso Fasano, Andrea Barra, Paola Nicosia, Federica Rinaldi, Pietro Bria, Anna Rita Bentivoglio, and Federico Tonioni. "Cocaine addiction: from habits to stereotypical-repetitive behaviors and punding". In: *Drug and alcohol dependence* 96.1-2 (2008), pages 178–182.

[30] Tanmay Nath, Alexander Mathis, An Chi Chen, Amir Patel, Matthias Bethge, and Mackenzie Weygandt Mathis. "Using DeepLabCut for 3D markerless pose estimation across species and behaviors". In: *Nature protocols* 14.7 (2019), pages 2152–2176.

[31] Kevin Luxem, Petra Mocellin, Falko Fuhrmann, Johannes Kürsch, Stephanie R Miller, Jorge J Palop, Stefan Remy, and Pavol Bauer. "Identifying behavioral structure from deep variational embeddings of animal motion". In: *Communications Biology* 5.1 (2022), pages 1–15.

[32] Alexander B Wiltschko, Tatsuya Tsukahara, Ayman Zeine, Rockwell Anyoha, Winthrop F Gillis, Jeffrey E Markowitz, Ralph E Peterson, Jesse Katon, Matthew J Johnson, and Sandeep Robert Datta. "Revealing the structure of pharmacobehavioral space through motion sequencing". In: *Nature neuroscience* 23.11 (2020), pages 1433–1443.

[33] Fangmiao Sun, Jingheng Zhou, Bing Dai, Tongrui Qian, Jianzhi Zeng, Xuelin Li, Yizhou Zhuo, Yajun Zhang, Yipan Wang, Cheng Qian, Ke Tan, Jiesi Feng, Hui Dong, Dayu Lin, Guohong Cui, and Yulong Li. "Next-generation GRAB sensors for monitoring dopaminergic activity in vivo". In: *Nature methods* 17.11 (2020), pages 1156–1166. DOI: 10.1038/s41592-020-00981-9.

[34] Miao Jing, Yuexuan Li, Jianzhi Zeng, Pengcheng Huang, Miguel Skirzewski, Ornela Kljakic, Wanling Peng, Tongrui Qian, Ke Tan, Jing Zou, et al. "An optimized acetylcholine sensor for monitoring in vivo cholinergic activity". In: *Nature methods* 17.11 (2020), pages 1139–1146.

[35] Zhi-Min Zhang, Shan Chen, and Yi-Zeng Liang. "Baseline correction using adaptive iteratively reweighted penalized least squares". In: *Analyst* 135.5 (2010), pages 1138–1146.

[36] Kaiming He, Xiangyu Zhang, Shaoqing Ren, and Jian Sun. "Deep residual learning for image recognition". In: *Proceedings of the IEEE conference on computer vision and pattern recognition*. 2016, pages 770–778.

[37] Jeffrey E Markowitz, Winthrop F Gillis, Celia C Beron, Shay Q Neufeld, Keiramarie Robertson, Neha D Bhagat, Ralph E Peterson, Emalee Peterson, Minsuk Hyun, Scott W Linderman, et al. "The striatum organizes 3D behavior via moment-to-moment action selection". In: *Cell* 174.1 (2018), pages 44–58.

[38] Terry E Robinson, Phillip A Jurson, Julie A Bennett, and Kris M Bentgen. "Persistent sensitization of dopamine neurotransmission in ventral striatum (nucleus accumbens) produced by prior experience with (+)-amphetamine: a microdialysis study in freely moving rats". In: *Brain research* 462.2 (1988), pages 211–222.

[39] Venus N Sherathiya, Michael D Schaid, Jillian L Seiler, Gabriela C Lopez, and Talia N Lerner. "GuPPy, a Python toolbox for the analysis of fiber photometry data". In: *Scientific reports* 11.1 (2021), pages 1–9.

[40] Weston Fleming, Junuk Lee, Brandy A Briones, Scott S Bolkan, and Ilana B Witten. "Cholinergic interneurons mediate cocaine extinction in male mice through plasticity across medium spiny neuron subtypes". In: *Cell Reports* 39.9 (2022), page 110874.

[41] Antonio Pisani, Paola Bonsi, Diego Centonze, Paolo Calabresi, and Giorgio Bernardi. "Activation of D2-like dopamine receptors reduces synaptic inputs to striatal cholinergic interneurons". In: *Journal of Neuroscience* 20.7 (2000), RC69–RC69.

5 Supplementary Figures

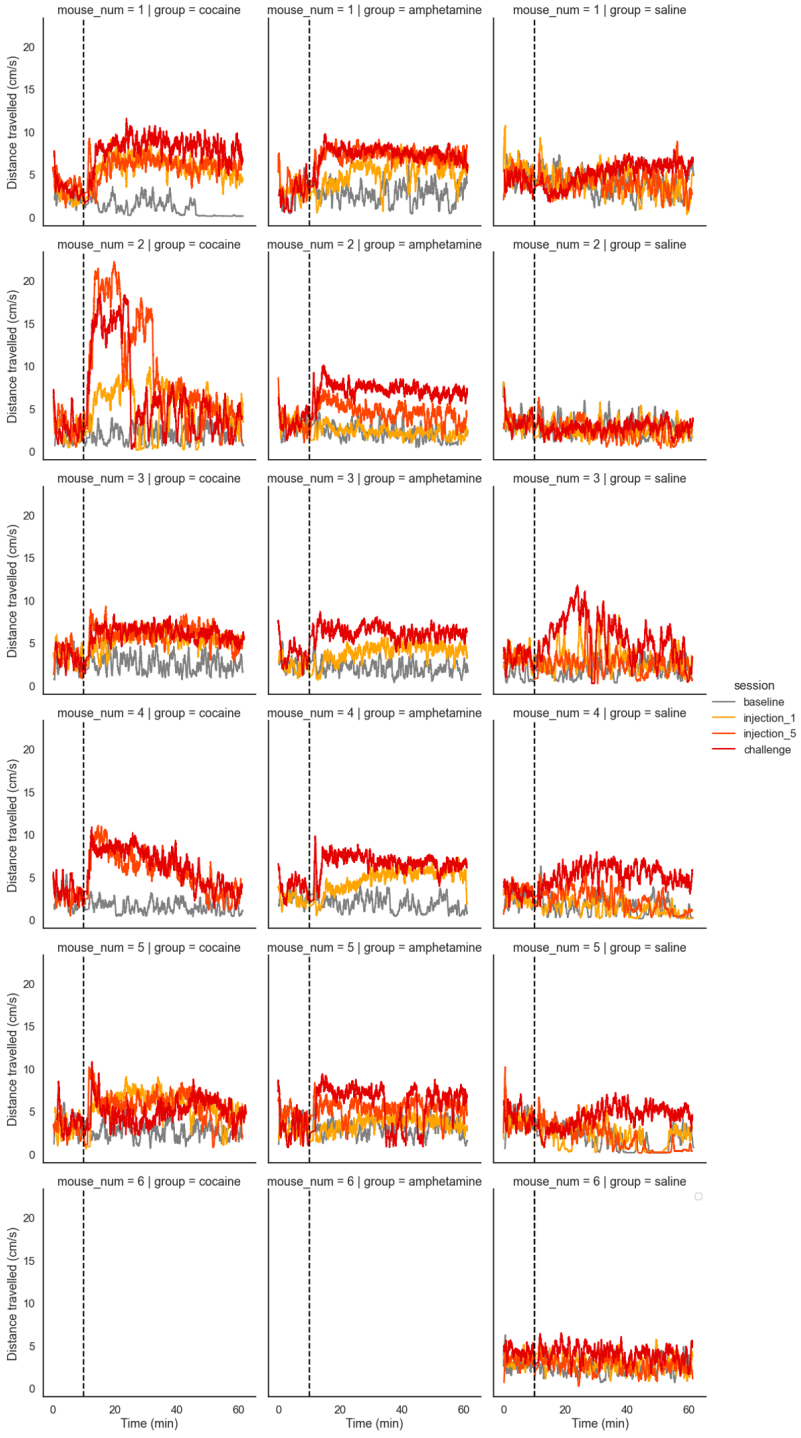

Figure 5.1: Locomotor activity per animal

Speed is measured at the base of the tail and averaged by a 60 second moving average. Every animal is represented in a different graph, color denotes the session. There are five animals for cocaine and amphetamine, and six in the saline group. Animals of the saline group received cocaine or amphetamine during the challenge recording. Injection 1 for animal C4 was excluded from all analyses because of a complication during the recording.

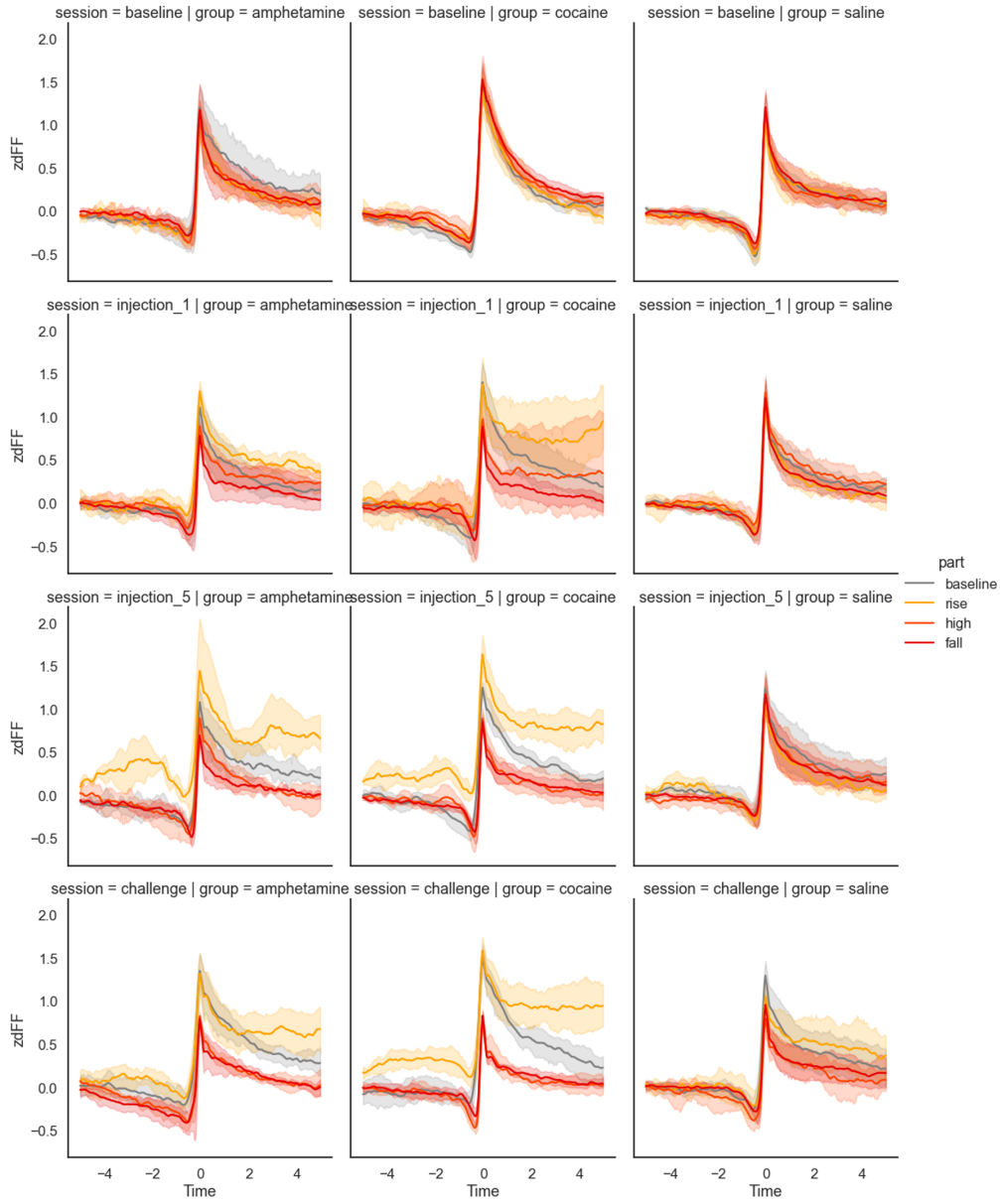

Figure 5.2: Dopamine Transients during Sensitization per Group and Session Shows dopamine traces around detected dopamine transients split by group and session. Individual plots are split in color by time when the transient occured: 10-0 minutes before injection for baseline, < 5 min for rise, 5 - 20 min for high and 20 - 50 min for fall. Individual transients of each animal were first averaged and then averaged again with the averages of the other animals. Errorbars show the standard error of mean with respect to the averages of the mice.

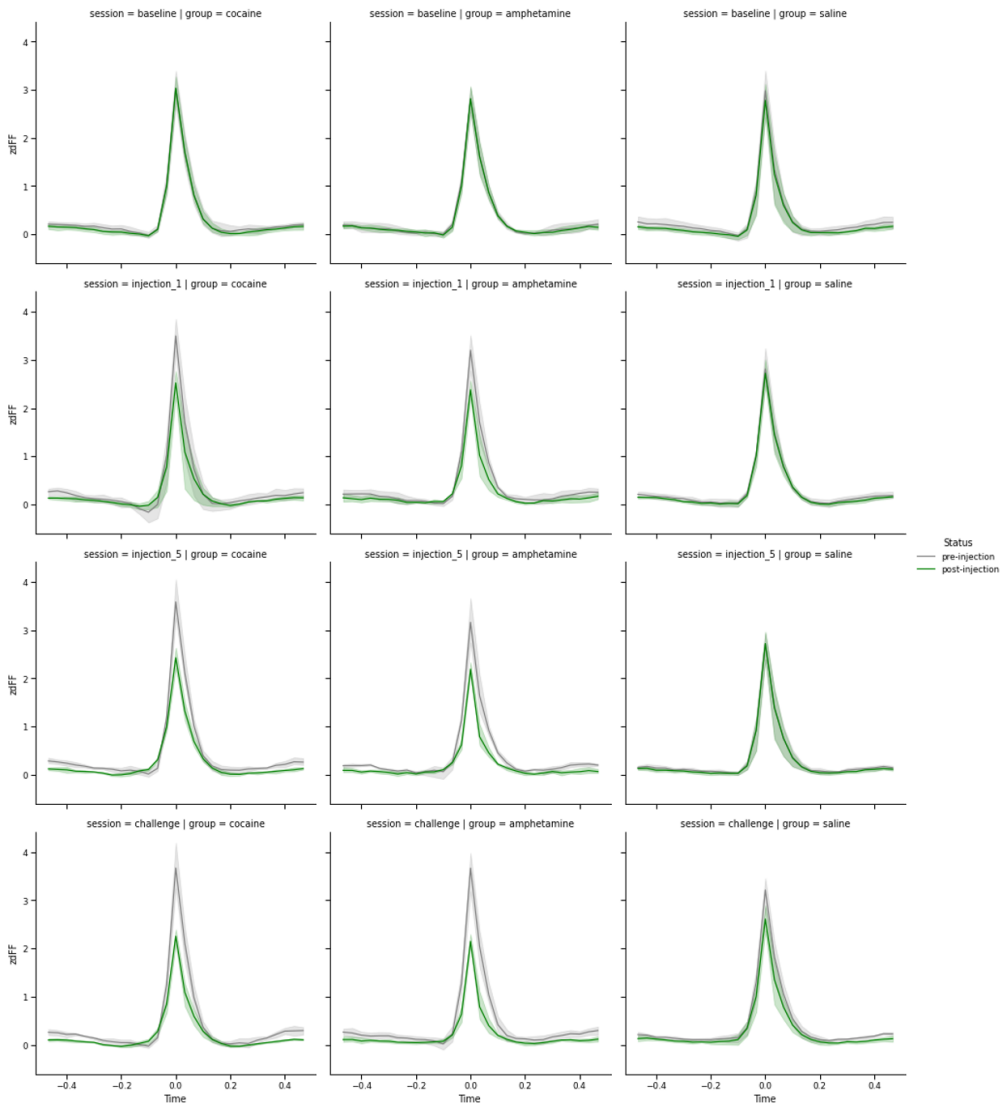

Figure 5.3: ACh transients decrease after injection of psychostimulants and during sensitization Data is separated vertically by session and horizontally by group. Each plot shows averaged ACh traces time-locked to ACh events and separated into events that occured during the 10 minute baseline (grey) and after injection (green)

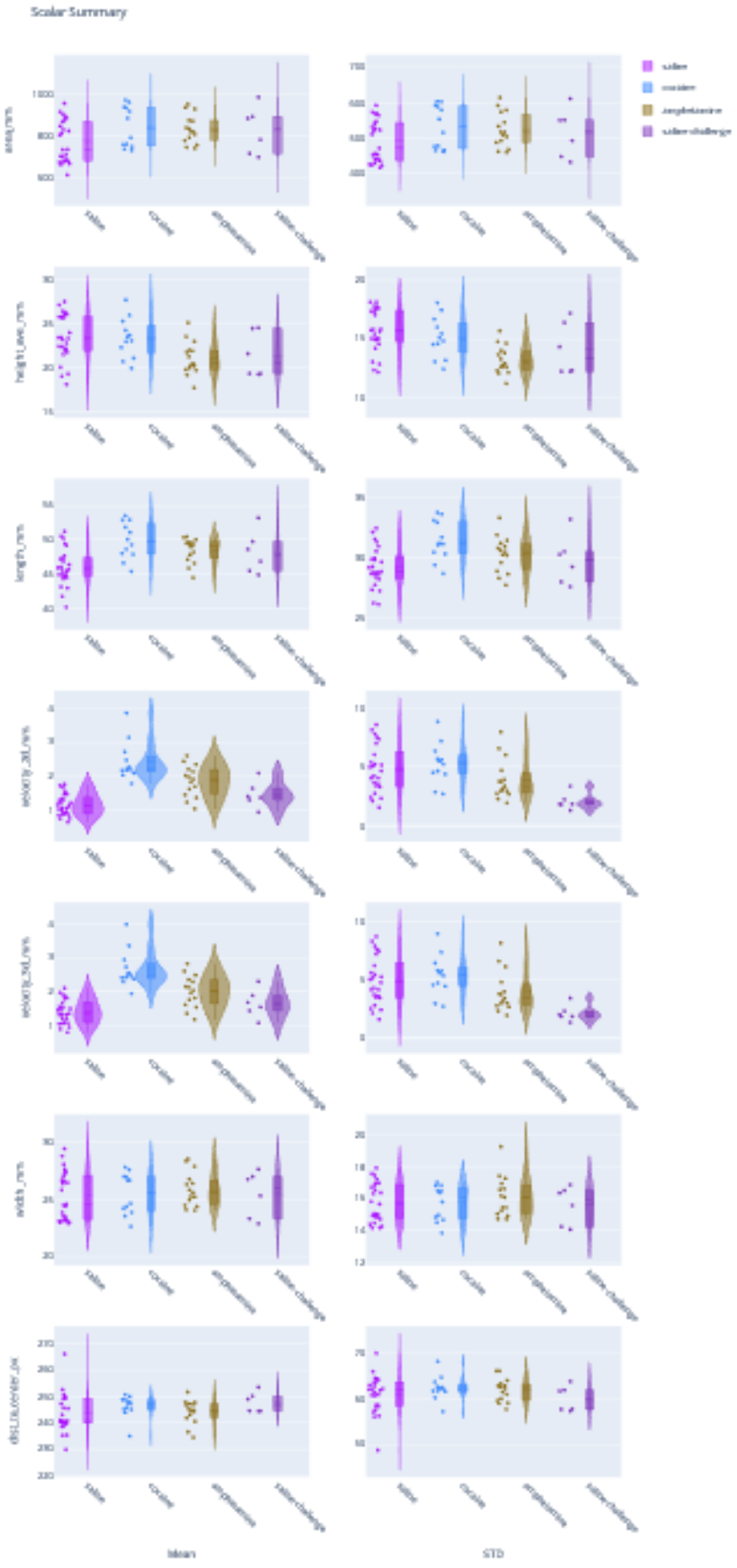

Figure 5.4: Statistics of extracted animals Graph shows different measurements collected of each animal and shows that extraction results are similar for every animal.

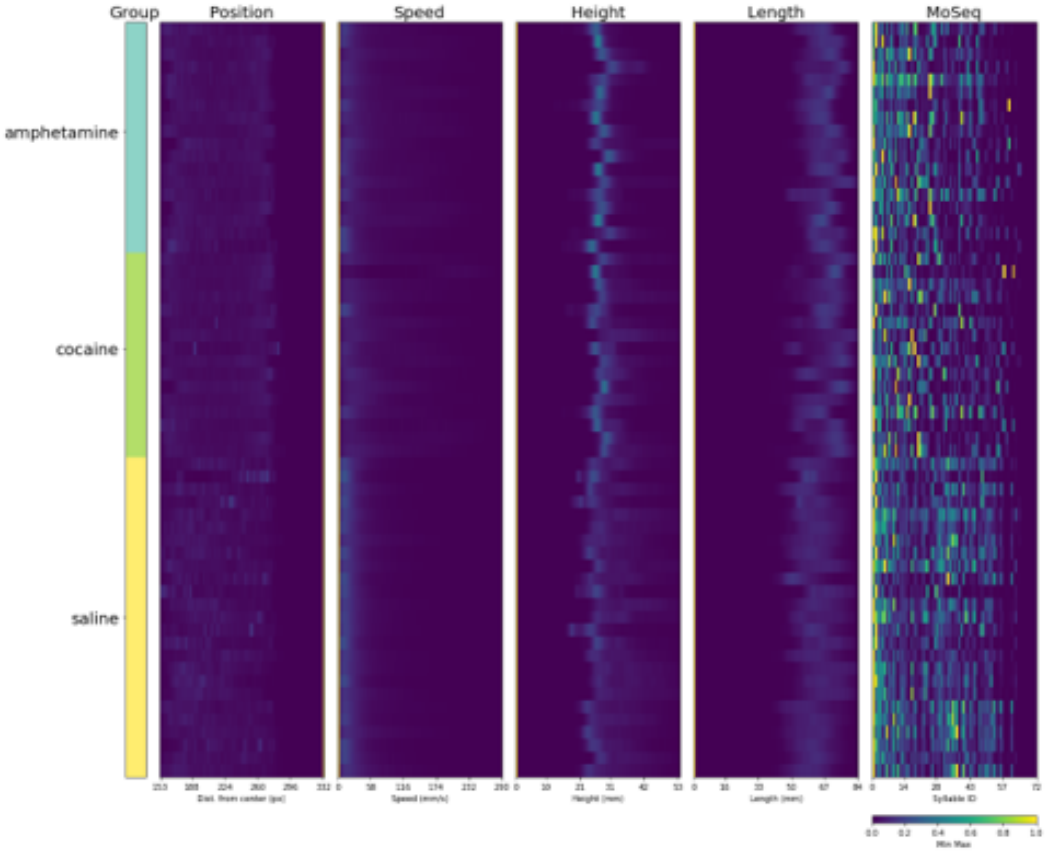

Figure 5.5: Fingerprints of all sessions Shown are position speed, height, length, and syllable usage for all sessions. Group denotes the substance that was injection during that respective session, not the experimental group

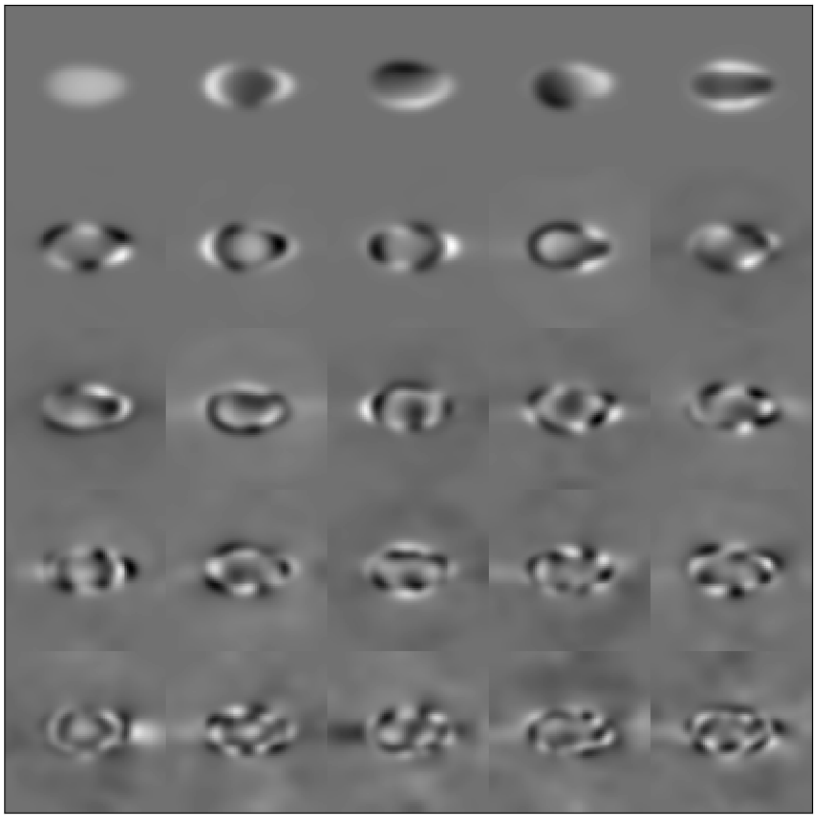

Figure 5.6: Principal Components

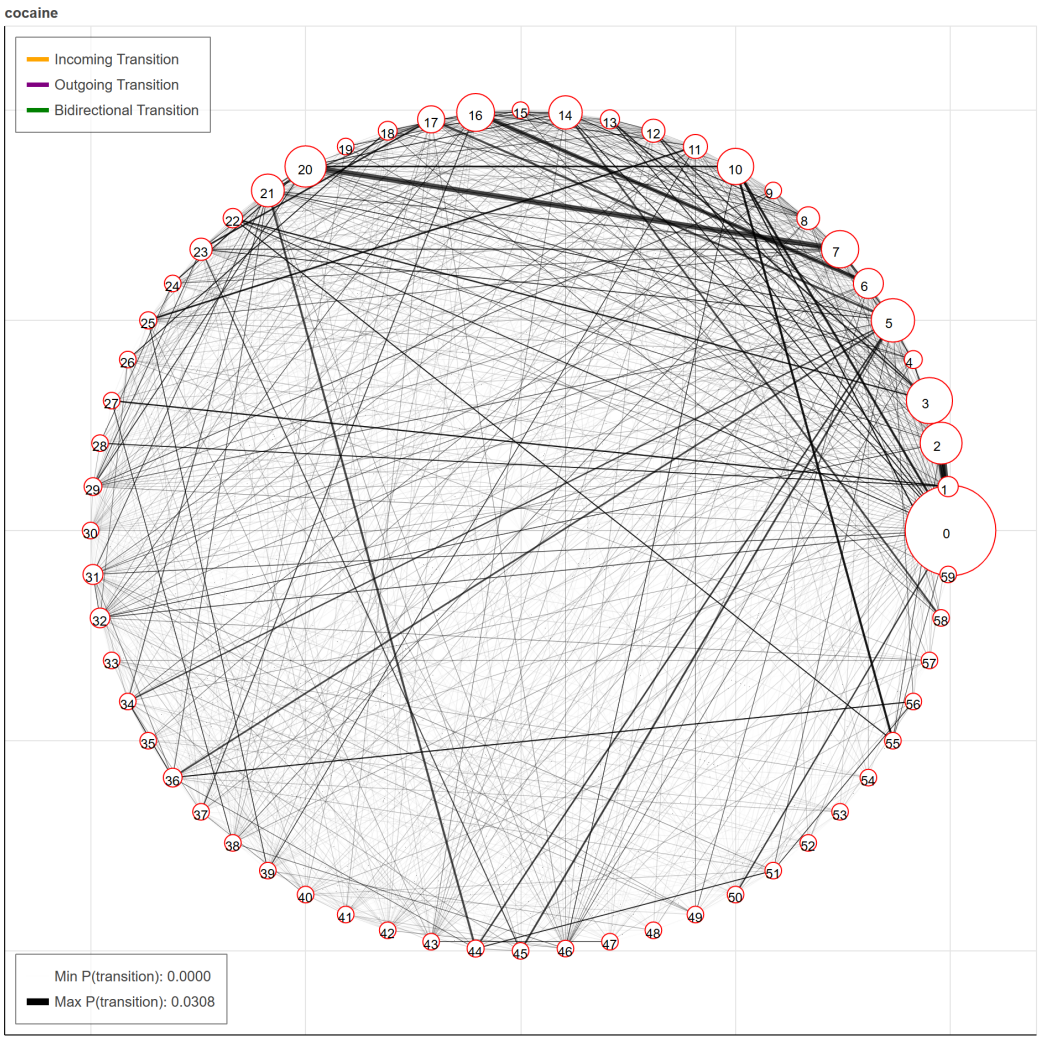

Figure 5.7: Syllable usage and transition probability for cocaine

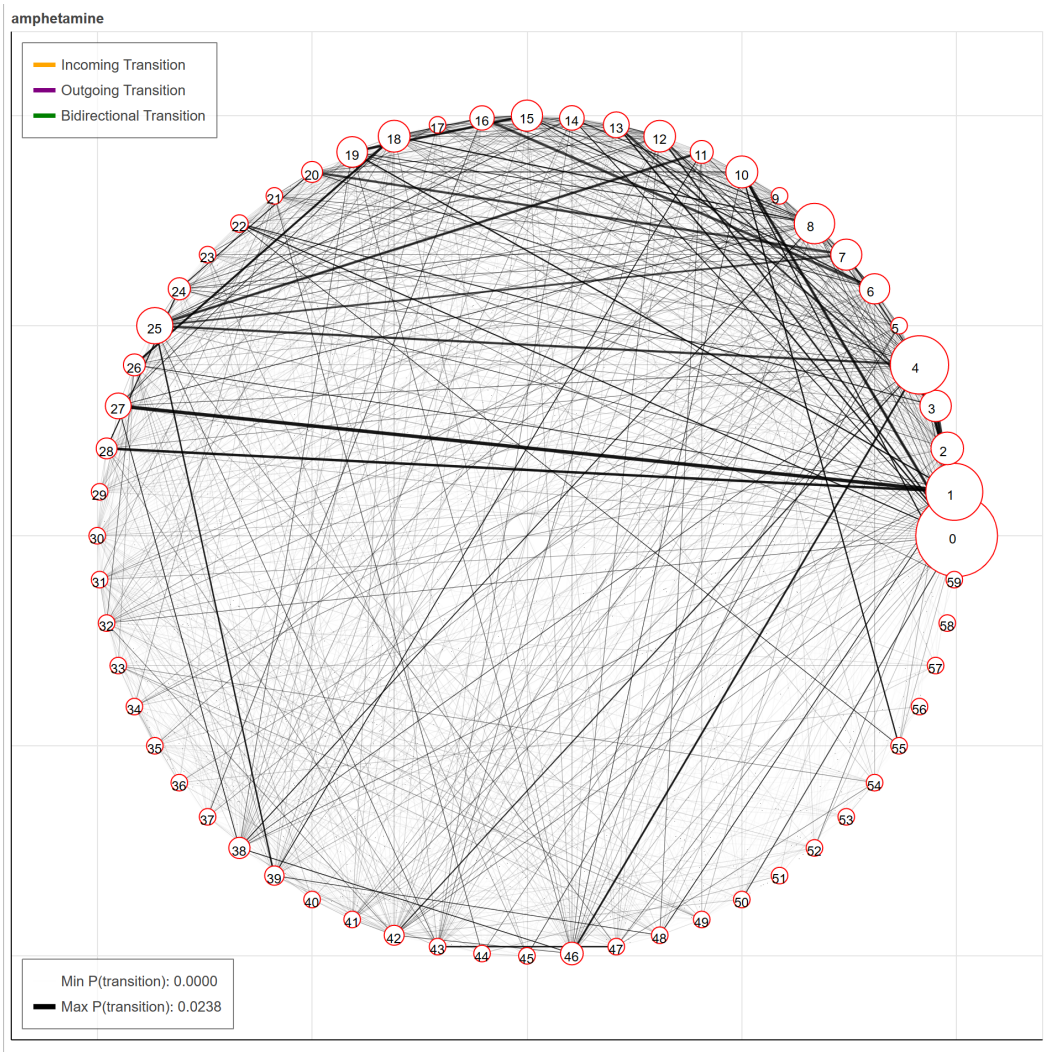

Figure 5.8: Syllable usage and transition probability for amphetamine

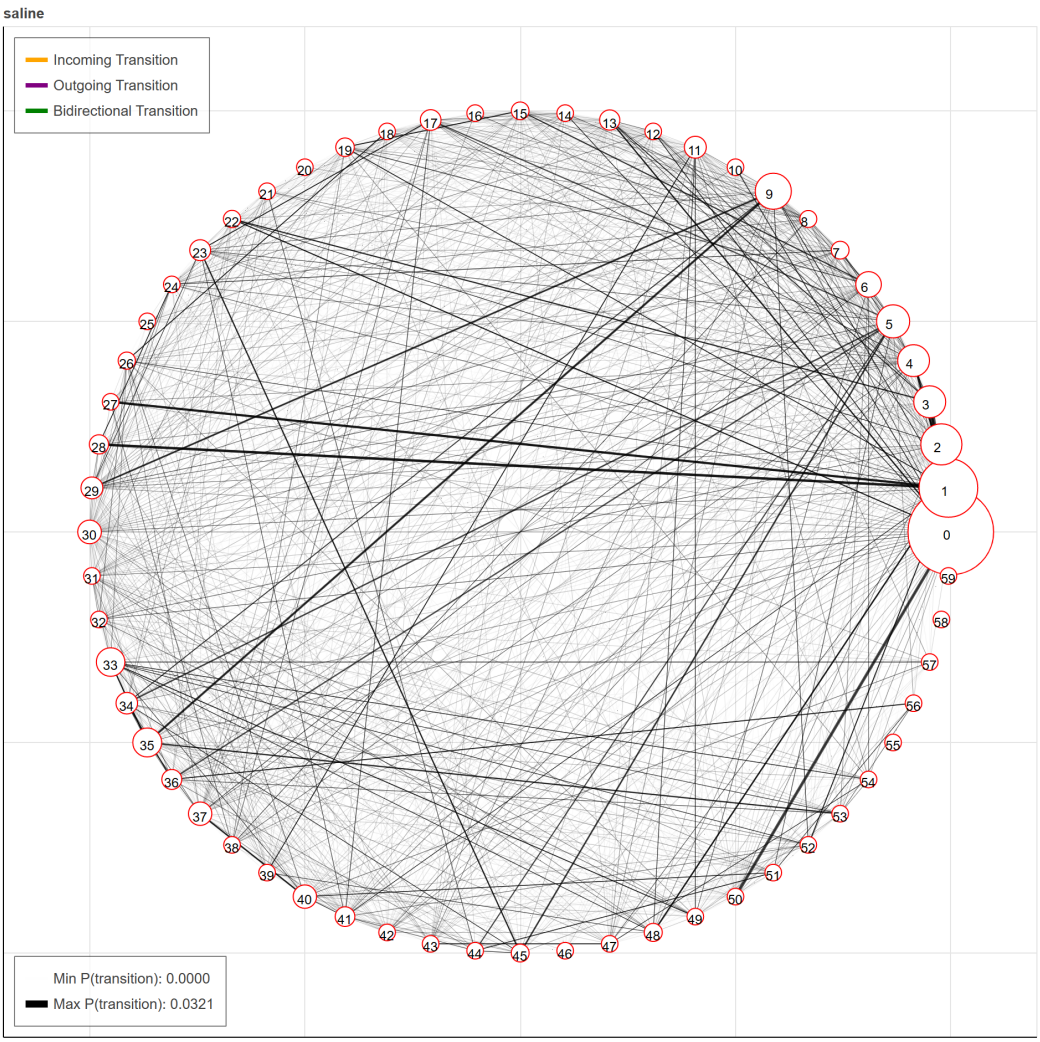

Figure 5.9: Syllable usage and transition probability for saline

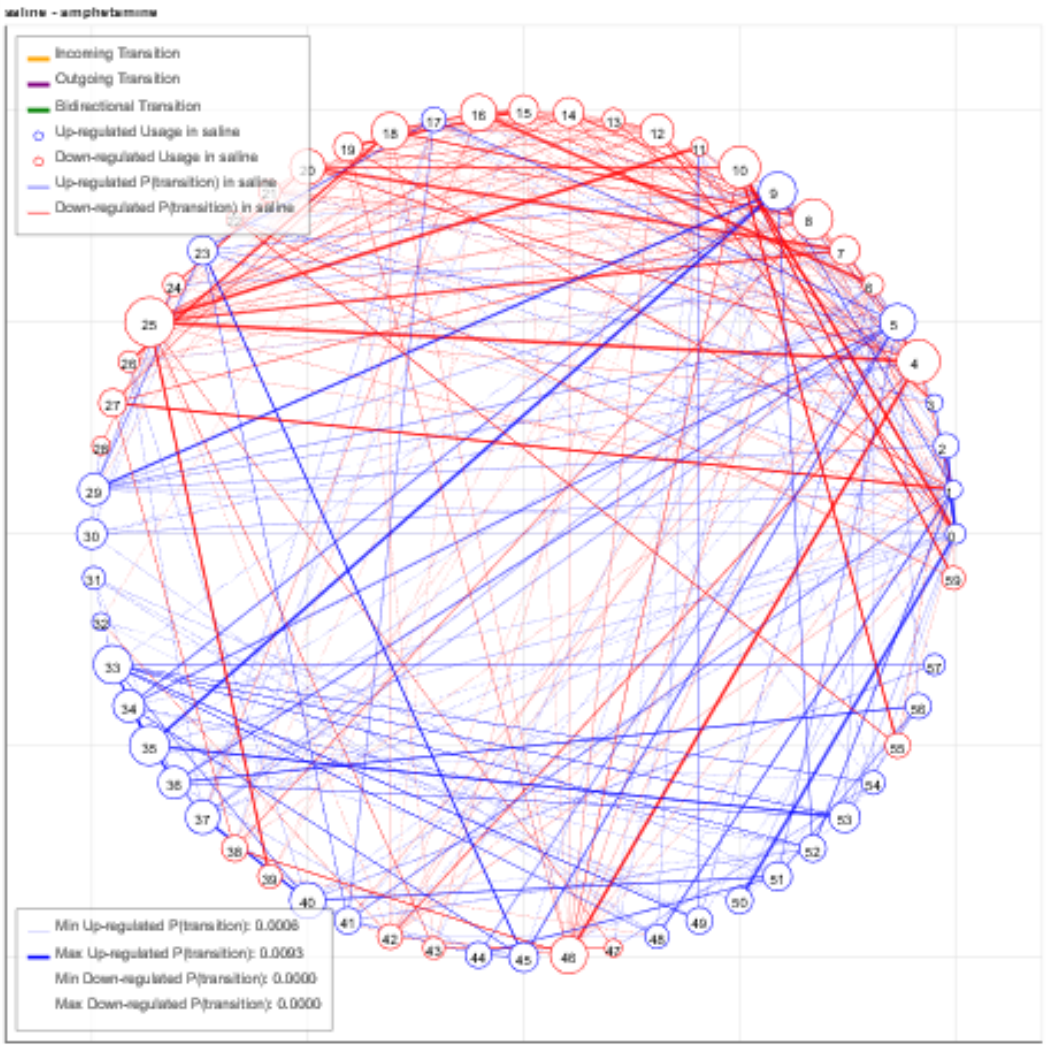

Figure 5.10: Difference in syllable usage and transition probability between amphetamine and saline

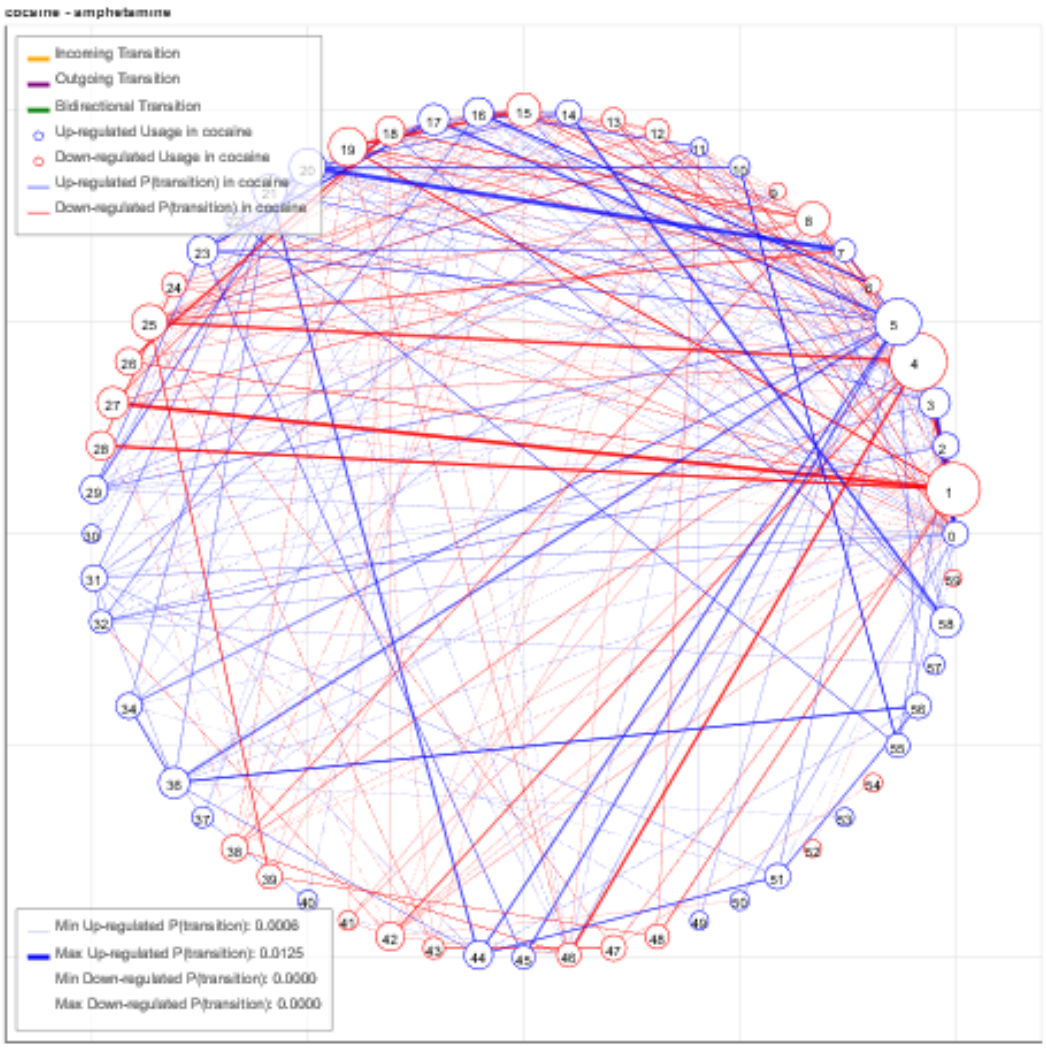

Figure 5.11: Difference in syllable usage and transition probability between amphetamine and cocaine